OPTIMIZATION OF THE DIAMETER AND WATER ABSORPTION CAPACITY OF SUPERABSORBENT POLYMER BEADS FOR THREE-DIMENSIONAL FILTRATION

A Dissertation
Presented to
The Academic Faculty

by

Shui Jing

In Partial Fulfillment
of the Requirements for the Degree
Master of Science in the
School of Civil and Environmental Engineering

Georgia Institute of Technology
December 2018

OPTIMIZATION OF THE DIAMETER AND WATER ABSORPTION CAPACITY OF SUPERABSORBENT POLYMER BEADS FOR THREE-DIMENSIONAL FILTRATION

Approved by:

Dr. Xing Xie, Advisor
School of Civil and Environmental Engineering
Georgia Institute of Technology

Dr. Sotira Yiacoumi
School of Civil and Environmental Engineering
Georgia Institute of Technology

Dr. Yongsheng Chen
School of Civil and Environmental Science
Georgia Institute of Technology

Date Approved: December 03, 2018

ACKNOWLEDGEMENTS

Thank you to my supervisor, Dr Xing Xie, for providing guidance and directing my focus throughout the project. Thanks to all the group members of the lab for their experimental and technical knowledge. I would like to thank Heying Liu and Weiling Yuan for assisting me in the experimental part, and thank Thomas Igou for preparing the algae solution.

To my parents and friends, thanks for supporting me and the confidence instilled in me.

TABLE OF CONTENTS

ACKNOWLEDGEMENTS **iii**

LIST OF TABLES **vi**

LIST OF FIGURES **vii**

LIST OF SYMBOLS AND ABBREVIATIONS **x**

SUMMARY **xi**

CHAPTER 1. INTRODUCTION **1**

CHAPTER 2. BACKGROUND **3**
2.1 Superabsorbent Polymers (SAPs) **3**
2.1.1 Classification 3
2.1.2 Production 4
2.1.3 Swelling Mechanism and Kinetics 4
2.2 Applications of SAPs **5**
2.3 SAP Beads **6**
2.4 Research Questions **8**
2.5 Research Objectives **8**

CHAPTER 3. RESEARCH METHODS **9**
3.1 Materials for SAP Beads **9**
3.2 The Synthesis of SAP Beads **10**
3.3 Synthesis of SAP Beads with Different Compositions **11**
3.3.1 SAP Beads with Different Crosslinking Degrees 11
3.3.2 SAP Beads with Different Monomer Ratios 12
3.3.3 SAP Beads with Different pH 13
3.4 Synthesis of SAP Beads with Different Diameters **14**
3.5 Characterization of SAP Beads **16**
3.5.1 Microscopy Images 16
3.5.2 Swelling Behaviors 16
3.5.3 Reusability 17
3.6 SAP Beads for Concentrating *E. coli* in Water **17**
3.7 SAP Beads for Harvesting Algae in Water **18**

CHAPTER 4. RESULTS AND DISCUSSIONS **20**
4.1 Effect of Composition on the Water Absorbency of SAP Beads **20**
4.1.1 Effect of Crosslinking Degree 20
4.1.2 Effect of AA to AM Ratio 22
4.1.3 Effect of pH 22
4.2 Products of SAP Beads with Different Sizes and Compositions **24**

4.3 Properties of the SAP Beads **28**
4.3.1 Surface Morphology 28
4.3.2 Sweling Behaviors 29
4.3.3 Water Absorbency under Different Ionic Strengths 34
4.3.4 Reusability 37
4.4 *E. coli* Concentrating **38**
4.5 Algae Harvesting **42**

CHAPTER 5. CONCLUSIONS **44**

REFERENCES **46**

LIST OF TABLES

Table 1	- Inner and outer diameters information for glass tubes from different vendors.	14
Table 2	- Dimensions information for different T junctions.	15
Table 3	- Dry bead sizes produced by glass tubes with different inner diameters.	24
Table 4	- Products of beads with different diameters and compositions.	27
Table 5	- Production of nine types of beads with different diameters and water absorbency.	34
Table 6	- Water absorbency for SAP beads with different crosslinking degree in deionized and saline water.	37
Table 7	- Dependency of water absorbency decreasing rate for beads on diameters.	38
Table 8	- Summary of the average and cumulative recovery efficiencies for the three concentrations tests.	41

LIST OF FIGURES

Figure 1	- Schematic diagram for sample concentration process using SAP beads. Adapted from "Nanofiltration enabled by superabsorbent polymer beads for concentrating microorganisms in water samples," by Xing Xie, Janina Bahnemann, Siwen Wang, Yang Yang, Michael R. Hoffmann, 2016, *Scientific Report*, 6, 20516.	2
Figure 2	- Fabrication and characterization of poly (AM-co-IA) beads. (a) Schematic of the fabrication procedure using millifluidic system. (b) The polymerization reaction for IA with AM. (c) The size change of poly (AM-co-IA) beads in DI water. Adapted from "Nanofiltration enabled by superabsorbent polymer beads for concentrating microorganisms in water samples," by Xing Xie, Janina Bahnemann, Siwen Wang, Yang Yang, Michael R. Hoffmann, 2016, *Scientific Report*, 6, 20516.	7
Figure 3	- Molecular formula of different monomers and reaction mechanism. (a) Molecular formula for itaconic acid (IA), acrylic acid (AA), and acrylamide (AM). (b) The polymerization reaction for AA with AM. Adapted from "Modified chitosan superabsorbent hydrogels from poly (acrylic acid-co-acrylamide) grafted chitosan with salt and PH responsiveness properties," by G.R. Mahadavinia, M.J. Zohuriaan, et al, 2004, *European Polymer Journal*, 40, 1399-1407.	9
Figure 4	- Fabrication of poly (AM-co-AA) beads. (a) Schematic of the fabrication procedure using two-step method. (b) Photo of the real structure.	11
Figure 5	- T junctions. (a) Design of T junctions. (b) Solidworks image of a T junction. (c) final product of a T junction.	15
Figure 6	- Effect of crosslinking degree and dilution on water absorbency of the beads.	21
Figure 7	- Crosslinking and cyclization reactions. Adapted from "Structure and swelling of poly (acrylic acid) hydrogels: effect of pH, ionic strength, and dilution on the crosslinked polymer structure," by Jeannine E. Elliott, Mara Macdonald, Jun Nie, Christophern. Bowman, 2004, *Polymer*, 45, 1503-1510.	21
Figure 8	- Effect of monomer AA/AM ratio on the absorbency of SAP beads.	22
Figure 9	- Effect of pH on beads swelling behavior.	23

Figure 10 - Images of SAP beads with different sizes. (a-c) SAP beads prepared by ID 1.5 mm glass tube; (d-f) SAP beads prepared by ID 0.8 mm glass tube; (g-i) SAP beads prepared by ID 0.5 mm glass tube; and (j-l) SAP beads prepared by inverse suspension polymerization. The left column, middle column, and right column of the images were taken by Digital View, a Zeiss advanced microscope, and iphone, respectively. 26

Figure 11 - Size distribution of SAP beads synthesized by inverse suspension polymerization. 27

Figure 12 - Scanning electron microscope (SEM) images of the outer surface of beads taken by Hitachi SU8010. 28

Figure 13 - Scanning electron microscope (SEM) images of the outer surface of beads taken by Zeiss Ultra60 FE-SEM. 29

Figure 14 - Size change of the SAP beads when soaking in DI water. (a) Beads with a 0.3 mm dry diameter. (b) Beads with a 0.5 mm dry diameter. (c) Beads with a 1 mm dry diameter. 30

Figure 15 - Swelling behavior comparison between SAP beads with different sizes. (a) Dependency of size change on time for beads with different diameters. (b) First-order swelling kinetics for beads. 32

Figure 16 - Swelling behavior comparison between SAP beads with different crosslinking degrees. (a), (c), and (e) Dependency of size change on time for beads with 1.0 mm, 0.5 mm, and 0.3 mm diameter and different crosslinking degrees. (b), (d), and (f) Corresponding first-order swelling kinetics for different beads. 33

Figure 17 - Effect of ionic strength of solution on the water absorbency of SAP beads. (a) and (c) Dependency of water absorbency on time for beads with 0.3 mm, 0.5 mm diameter respectively and 0.25 wt% of crosslinker in NaCl solutions with different concentrations. (b) and (d) Dependency of water absorbency on solution ionic strength for beads with 0.3 mm, 0.5 mm diameter respectively and different crosslinking degree. 35

Figure 18 – Swelling behavior of 0.3 mm SAP beads in 10 g/L NaCl solution. 36

Figure 19 - Reusability of SAP beads. (a) Water absorbency of beads when recycled with different crosslinking degrees. (b) Water absorbency of beads when recycled with different sizes. 38

Figure 20 - Performance of applying SAP beads to concentrate *E. coli* microorganisms. (a), (b) and (c) in different initial concentrations: 3.0×10^2 CFU/mL, 2.1×10^3 CFU/mL, and 6.7×10^3 CFU/mL 41

respectively. (d) Summary of the average and cumulative recovery efficiencies for the three concentrations tests.

Figure 21 - Recovery efficiencies of a single concentrating step with different concentration degrees. 42

Figure 22 - Performance of applying SAP beads to harvest microalgae in solution. (a) Comparison between measured and theoretical concentrations of algae in each step. (b) Recovery efficiency decreases in each step. 43

LIST OF SYMBOLS AND ABBREVIATIONS

SAP	Superabsorbent polymer
AM	Acylamide
AA	Acrylic acid
W/O	Water-in-oil
KPS	Potassium persulfate
MBA	N,N’-methylene bisacylamide
IA	Itaconic acid

SUMMARY

The filtration process has been widely used in various industrial applications. To offer more interfacial area and promote the efficiency for the filtration process, a three-dimensional filtration process based on superabsorbent polymer (SAP) beads has been developed. Here in this study, a new two-step polymerization method was established to synthesize (acrylamide-co-acrylic acid) (AM-co-AA) SAP beads. Using this method, SAP beads with three different diameters (0.3 mm, 0.5 mm, and 1.0 mm) were produced. The composition of SAP beads was thoroughly studied. The molar ratio of the two monomers, the total concentration of the monomer solution, the pH of the monomer solution, and the crosslinking degree have significant effects on the water absorbency of SAP beads. After the composition study, SAP beads with three different water absorbencies (around 100, 300, and 500) were produced. The swelling behavior of each type of beads were studied by soaking in DI water or salt (NaCl) solution. According to the result of the study, beads with smaller size swell faster than beads with larger size and reach equilibrium in a shorter time. Although SAP beads with a lower crosslinking degree obtain a higher water absorbency, they need longer time to reach equilibrium when beads have the same size. Meanwhile, SAP beads with a high crosslink density have a greater longevity when recycled. The swelling performance of beads in salt solution was diminished due to the decreased osmotic pressure. Typically, the water absorbency for beads with a 0.5 mm diameter decreased from 466 in DI water to 141 when the ionic strength increased to 0.02 mol/L. SAP beads were applied in the *E. coli* concentration and algae harvesting

experiments. The results of these two experiments demonstrate that SAP beads show good recovery efficiency and can be applied to other potential applications.

CHAPTER 1. INTRODUCTION

The water filtration process is technically defined as the separation of suspended solids from water [1]. By gravity or pressure, water passes through the pores of a membrane, which is also referred as filter, while particles are collected or excluded. The fluid that passes through is called the filtrate. According to the size of excluded particles, filtration can be classified into different categories. For example, the typical size for microfiltration ranges from 0.1-10 μm; nanofiltration ranges from 1-10 nm. Filtration has been widely applied to food, pharmaceutical, chemical industries to remove contaminants or harvest products [2-4].

Darcy's law is an equation describing the flow when it passes through a porous medium, which can be applied to the filtration process [5]. The equation is shown below:

$$Q = -\frac{\kappa A(P_1 - P_2)}{\mu L}$$

where Q, the total flow rate (m^3/s), is the product of intrinsic permeability κ (m^2), the area A (m^2), the pressure difference divided by the viscosity μ and the length L. According to the equation, it is obvious that the total flow rate is proportional to the total area. Therefore, to promote the efficiency and offer substantially more interfacial area is critical for the filtration process.

Compared with the traditional 2D filtration with a whole porous membrane, the new 3D filtration composed of multiple individual sphere units has larger surface area to volume ratio. Therefore, this more effective process was achieved by using superabsorbent polymer

(SAP) beads. Figure 1 shows the water filtration process with SAP beads [6]. Dry beads are added to the original sample and swell until equilibrium is reached. Then, the beads are separate from the water sample. During the process, target particles are excluded in the residual. After beads are dehydrated and dried, they are collected and reused.

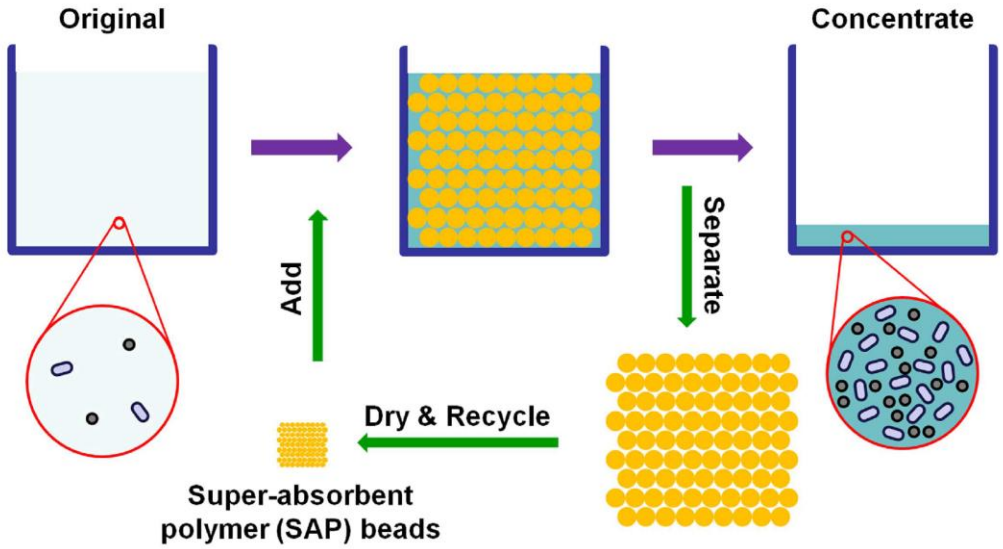

Figure 1 - Schematic diagram for sample concentration process using SAP beads. Adapted from "Nanofiltration enabled by superabsorbent polymer beads for concentrating microorganisms in water samples," by Xing Xie, Janina Bahnemann, Siwen Wang, Yang Yang, Michael R. Hoffmann, 2016, *Scientific Report*, 6, 20516.

This 3D filtration based on SAP beads have several advantages over traditional filtration method in many aspects: 1) the contact area is significantly enlarged in a limited space; 2) the overall time requirement for a filtration process no longer depends on the volume of the water sample. If a large volume of water sample needs to be filtered, more SAP beads can be added to the sample; 3) no equipment is involved in the filtration process; 4) SAP beads are cheap and reusable, promising for future scale-up.

CHAPTER 2. BACKGROUND

2.1 Superabsorbent Polymers (SAPs)

Hydrogel is defined as a polymeric material that can absorb and retain large amount of water. This property arises from its unique structure where functional groups attached to the polymeric backbones absorb water and the cross-links between network chains prevent the hydrogel from dissolution [7]. Superabsorbent polymers (SAPs), belonging to the hydrogels but relatively lightly crosslinked, can absorb deionized water up to 1000 g/g [8]. The first commercial SAP was developed in Japan in 1978 for feminine napkins and in US in 1980 for baby diapers [9]. The production capacity of SAPs was more than 3 million tons per year in 2016 [10].

2.1.1 Classification

SAPs can be classified into two groups according to their origins: synthetic and natural. Natural SAPs do not have charged groups in the structure, including proteins such as collagen and polysaccharides such as starch. Usually, natural SAPs are prepared by adding some synthetic parts to the natural substrates. Synthetic SAP are prepared from monomers accompanying ionic charges. Based on the type of electrical charges on the monomer, SAPs can be further categorized into four groups: ionic, ampholytic, and zwitterionic. Most of the SAPs are anionic.

They also can be classified by the polymeric composition as a result of different methods of preparation: homopolymeric, copolymeric, and interpenetrating polymeric SAPs. Homopolymeric SAPs refer to networks that are formed by one type of monomer unit.

Copolymeric SAPs are crosslinked by two or more different monomer species, at least one of which is hydrophilic. Interpenetrating polymeric SAPs are composed of two independently crosslinked polymer components in one network. [11]

2.1.2 Production

In general, three essential ingredients including monomer, initiator, and cross-linker are used to synthesize SAPs. Acrylic acid (AA) and its sodium salt, and acrylamide (AM) are often used as monomers. Potassium persulphate (KPS) and ammonium persulphate (APS) are common thermal initiators. N, N'-methylene bisacrylamide (MBA) is often used as a water-soluble cross-linking agent.

Two polymerization techniques, solution polymerization and inverse-suspension polymerization, related with this research have been described here. The solution polymerization process is straight forward: all the ingredients are dissolved in water at desired concentrations; the reaction is initiated by thermal initiator under heat; gel-like product is formed. Inverse-suspension polymerization refers to a water-in-oil (W/O) process, where all ingredients are dispersed in the oil phase. The particle size and shape are controlled by the viscosity of the continuous phase, agitation speed, and the type of dispersant [12].

2.1.3 Swelling Mechanism and Kinetics

It is important to understand its kinetics of swelling behaviour before applying SAPs to use. Usually two steps are considered: water molecules diffuse into the structure of the polymer, followed by the relaxation of polymer chains [13].

When the system is controlled by the diffusion step, indicating that the solvent mobility is limited, and diffusion rate is lower than the relaxation rate, Fickian model can be applied. In this model, the absorbed water mass M_t per unit mass of the polymer at time t is expressed by the equation below:

$$M_{tF} = M_{\infty}\left[1 - \frac{6}{\pi^2}\sum_{n=1}^{\infty}\frac{1}{n^2}exp(-n^2kt)\right]$$

where M_{∞} is the total amount of water absorbed by the polymer at equilibrium, and $k = 4\pi^2 D/d^2$ is the diffusion rate constant for polymer with an equivalent diameter of d. D is the diffusivity.

When the relaxation phenomenon is considered, the absorbed water mass M_{tR} can be expressed by the following equation where k_i is the relaxation rate constant, related with the swelling tension.

$$M_{tR} = \sum_{i=1}^{iR} M_{\infty i}[1 - exp(-k_i t)]$$

Most often, the swelling behaviour is a combination of these two steps. Therefore, the total Mass M_t is expressed as $M_t = M_{tF} + M_{tR}$.

2.2 Applications of SAPs

SAPs have been widely produced all over the world while most of them are used in disposable diapers. To improve the quality of diapers, a new generation of Safe and Natural Absorbent Polymer (SNAP) has been invented which contains no residual monomer [14].

In the pharmaceutical area, one type of SAP called super-porous hydrogels (SPHs) was invented by Kinam Park et al [15], which was designed for gastric retention applications [16]. Compared with SAPs, SPHs swell fast regardless of their gel size due to the capillary force through the porous structure.

Considering the water absorption properties of SAPs, their applications in agricultural fields have been investigated in order to reduce the loss of water in soil. They can be seen as “miniature water reservoirs” in soil [17]. Water will be removed from SAPs according to the root demand. SAPs also can be used to control the release of nutrients and pesticides avoiding the contamination of groundwater [18].

SAPs has also been used in concrete to self-seal cracks by Buenfeld and his research group [19]. When cracks form, they are likely to propagate through SAP voids, resulting in the exposure of SAPs to the external environment. When the concrete is subjected to a wet face, SAPs swell again, preventing the further flow of water and assisting the self-healing process.

2.3 SAP Beads

Xie et al. has successfully synthesized poly (acrylamide-co-itaconic acid) (P(AM-co-IA)) SAP beads using a millifluidic system for 3D filtration [6]. In this work, water-in-oil droplets were generated when the water phase stream and the oil phase stream (silicone oil) were combined at the T junction, as shown in Figure 2a. The water phase contains acrylamide (AM), itaconic acid (IA), potassium persulfate (KPS), and N,N’-methylene bisacrylamide (MBA). Figure 2b shows the polymerization reaction mechanism of this process. Water-in-oil droplets flowed through the silicone tubing with an inner diameter

(ID) of 1/16 inch. Under certain amount of heat, monomers were polymerized, and beads were formed. Then beads were washed by ethanol and dried in oven at 40°C overnight.

The size of the dried beads was around 1.27 mm. They were soaked in deionized water to measure the water absorbency. As Figure 2c shows, the water absorbing process reached equilibrium in 10 minutes, and the diameter of beads was around 3.8-fold of its original value. Thus, the water absorbency was around 50 g water/g SAP.

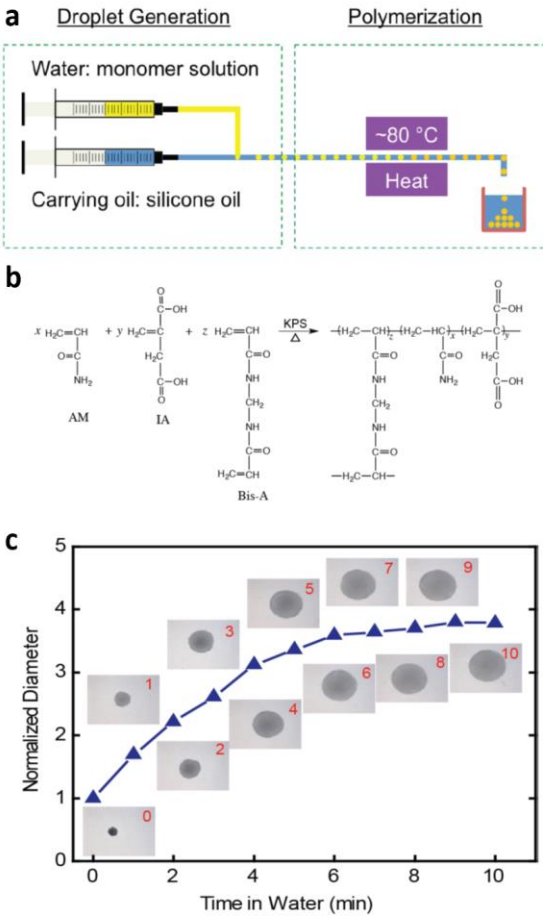

Figure 2 - Fabrication and characterization of poly (AM-co-IA) beads. (a) Schematic of the fabrication procedure using millifluidic system. (b) The polymerization reaction for IA with AM. (c) The size change of poly (AM-co-IA) beads in DI water. Adapted from "Nanofiltration enabled by superabsorbent polymer beads for concentrating microorganisms in water samples," by Xing Xie, Janina Bahnemann, Siwen Wang, Yang Yang, Michael R. Hoffmann, 2016, *Scientific Report*, 6, 20516.

2.4 Research Questions

One critical parameter is the diameter of the SAP beads. When the size of beads is smaller, it tends to absorb water much faster and reach equilibrium in less time because of its larger surface area to volume ratio. However, when the size of beads is too small, it is difficult to separate them from the residual water, which results in the decrease of separation efficiency.

It is desirable to produce beads with higher water absorbency that fewer SAP beads are needed to treat certain amount of water. However, the stiffness of beads decreases as the water content increases. When the water content is too high, beads may not be able to retain the integrity, increasing the difficulty of separating them from water.

Since the diameter, water absorbency, and stiffness of the beads are interrelated, how we optimize all the parameters during the synthetic process to achieve high water absorbency in a short time while also keep the separation efficiency is the question we need to address.

2.5 Research Objectives

The objectives of the research include: 1) establishing an improved synthetic method for preparing SAP beads; 2) elucidating the effect of composition on the swelling behavior of the SAP beads; 3) obtaining beads with desired water absorbency and stiffness; and 4) identifying the optimal diameter of the beads for future applications.

CHAPTER 3. RESEARCH METHODS

3.1 Materials for SAP Beads

The water phase contains acrylamide (AM) as a solid powder (99+%; Sigma-Aldrich), acrylic acid (AA) in liquid form (99%; Sigma-Aldrich), potassium persulfate (KPS) (99+%; Sigma-Aldrich), and N,N'-methylene bisacrylamide (MBA) (99%; Sigma-Aldrich). Itaconic acid (IA) used in the previous study was replaced by acrylic acid (AA). These two acids are all anionic and can be polymerized by free radical polymerization. Despite the structure of IA including two carboxyl groups, which may indicate a higher swelling ratio [20], it has a limited solubility in water at 0.2467 g/mL at 97°C [21] and lower reactivity than AA [22]. Chemical structures of the discussed monomers and the polymerization reaction are shown in Figure 3 [23].

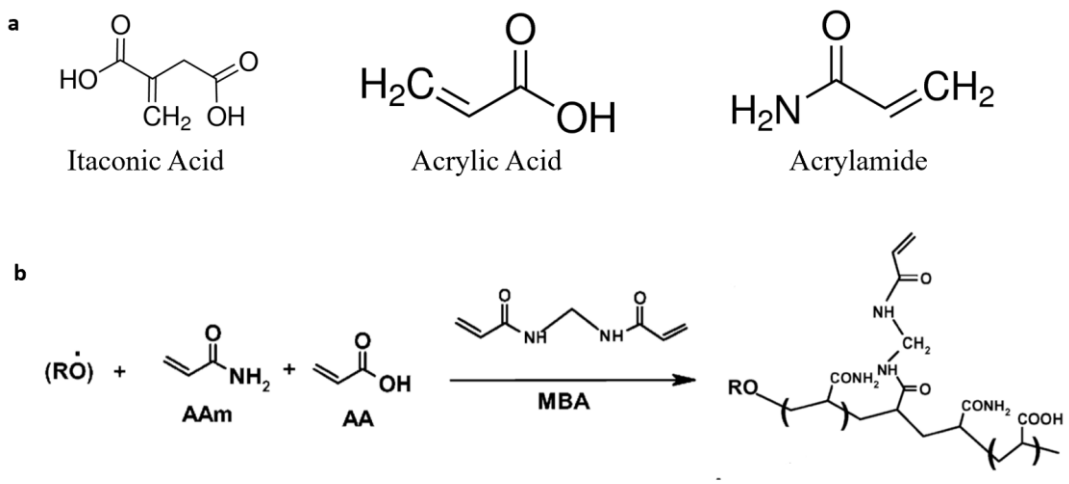

Figure 3 - Molecular formula of different monomers and reaction mechanism. (a) Molecular formula for itaconic acid (IA), acrylic acid (AA), and acrylamide (AM). (b) The polymerization reaction for AA with AM. Adapted from "Modified chitosan superabsorbent hydrogels from poly (acrylic acid-co-acrylamide) grafted chitosan with salt and PH responsiveness properties," by G.R. Mahadavinia, M.J. Zohuriaan, et al, 2004, *European Polymer Journal*, 40, 1399-1407.

AA (Sigma-Aldrich, 99%) cannot be used directly since it contains 200 ppm MEHQ as inhibitor to prevent it from converting to its dimer. Therefore, it was distilled under reduced pressure before use. [24]

3.2 The Synthesis of SAP Beads

In the previous method [6], aqueous droplets were polymerized under a certain temperature. Meanwhile, the reaction time should be long enough to ensure that the polymerization process is completed, otherwise the droplets may not be able to form solidified SAP beads. However, the lack of temperature and time control in this method is the primary concern. When the temperature given for the reaction is too low, complete polymerization requires longer time, i.e., longer silicone tube or slower flow rate, both of which may increase the possibility of the tube being blocked by SAP beads.

To overcome this problem, a two-step polymerization method was developed. As illustrated in Figure 4a, first of all, water-in-oil droplets were generated when the water phase stream and the oil phase stream were combined at a T junction. The oil phase was silicone oil. Two independent high-precision syringe pumps were applied to inject the streams. Second, droplets flowed through a dry bath with a temperature of 100°C for about 4 min. Then, partially polymerized SAP beads dropped to a beaker containing the same silicone oil and cured at 70°C for about 240 min. SAP beads were separated from oil by strainer or screen bags according to the size of beads. Last, beads were washed with DI water for a couple of minutes and dried in oven at 60°C overnight.

Silicone tube was substituted by glass tube since silicone tube deforms at 80°C in a long-term use and glass tube is highly resistant to temperature. Because the surface of glass tube

is hydrophilic, it needs to be modified to hydrophobic before use. When the surface is hydrophilic, the shape of aqueous droplets formed in the tube is columns rather than droplets. The higher contact areas also facilitate the blocking of the tube because droplets become sticky when they are polymerized.

The hydrophilic glass tube was modified by a surface treatment step. First, 0.2 mL methyltrichlrosilane and 0.5 mL concentrated hydrochloric acid (37% from Sigma Aldrich) were mixed in 20 mL toluene [25]. The mixture was injected into the glass tube by a syringe gradually. The glass tube was filled with the treatment solution for half an hour. After that, the glass tube was dried in oven at 60°C for 30 min.

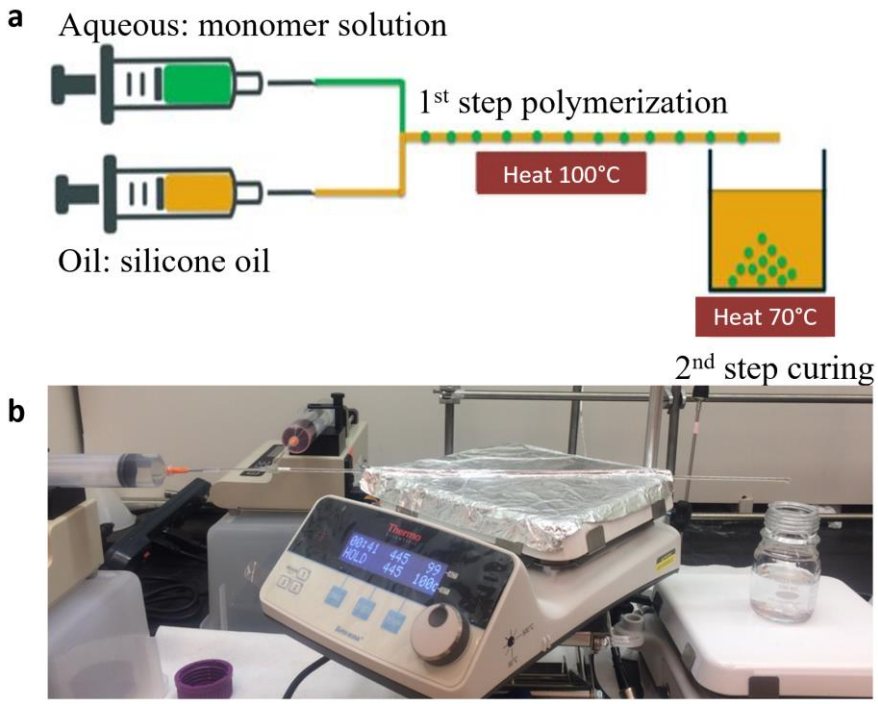

Figure 4 - Fabrication of poly (AM-co-AA) beads. (a) Schematic of the fabrication procedure using two-step method. (b) Photo of the real structure.

3.3 Synthesis of SAP Beads with Different Compositions

3.3.1 SAP Beads with Different Crosslinking Degrees

The degree of crosslinking in the SAP beads is critical because it determines the water absorbency as well as the mechanical strength of the SAP beads. Obviously, the degree of crosslinking is related to the percentage of cross-linker in the monomer mixture. However, the question remains what the critical percentage of crosslinker is to ensure SAP beads exhibit high water absorbency while also maintain the integrity.

The water absorbency is determined by the following expression [26]:

$$\text{water absorbency} = \frac{M_t - M_0}{M_0} \ (g/g\ beads)$$

where M_t and M_0 are the mass at different time-intervals and initial mass respectively.

To answer this question, two parallel experimental studies have been conducted. Each study has 5 parallel experiments. In the first study, the molar ratio of AM to AA was fixed at 4:1, and the total molar concentration of monomers was 3 mol/L. Meanwhile, the pH of the mixture was adjusted to 7 by NaOH solution. The amounts of KPS added to the monomer mixture was fixed at 1.5 wt% of the total weight of the monomers. The amount of MBA added was set as 0.05 wt%, 0.1 wt%, 0.25 wt%, 0.5 wt%, and 1.0 wt%. For the other study, excepting the total molar concentration, which was set to be 2 mol/L, other parameters were exactly the same. Mmonomer solution was sufficiently mixed until the solution was clear, and then heated on the hot plate at 70°C for 10 min. The polymerized gel was cut into cubes and dried in oven at 60°C overnight for future the test. To test the water absorbency of beads with different crosslinking degrees, completely dried cubes were soaked in DI water at ambient conditions for 1 hour.

3.3.2 SAP Beads with Different Monomer Ratios

Two monomers AA and AM were used as two basic monomers. AA contains -COOH group that can be ionized. Therefore, the ratio of AA to AM may change the swelling capability of beads. The AA to AM ratio of the reaction mixture was varied from 1/9 to 4 for different runs. Meanwhile, the total monomer concentration was kept the same at 2.5 mol/L. The amounts of KPS and MBA added to each monomer mixture were 1.5 wt% and 1.0 wt% respectively. Mmonomer solution was sufficiently mixed until the solution was clear, and then heated on the hot plate at 70°C for 10 min. The polymerized gel was cut into cubes and dried in oven at 60°C overnight for future the test. To test the water absorbency of beads with different crosslinking degrees, completely dried cubes were soaked in DI water at ambient conditions for 1 hour.

3.3.3 SAP Beads with Different pH

Acrylic acid (AA) contains carboxylic acid group, which is sensitive to pH. According to the literature, when the degree of neutralization increases from 4 to 7, the rate of polymerization increases significantly [27]. As the degree of neutralization increases, sodium acrylate forms. When the ratio of sodium carboxylate and carboxylic acid groups varies, the water absorbency will change. Therefore, we need to find the best neutralization degree or pH value to maximize the amount of water that SAP beads can absorb.

The monomer mixture was prepared in a glass bottle by mixing certain amounts of AM, AA, KPS, and MBA. Then the 160 mL mixture solution was equally devided into 8 samples that each sample contained 20 mL monomer solution. Pre-determined amounts of high concentration NaOH solution was added to each tube drop by drop until the pH reached 3, 4, 5, 6, 7, 8, 10, 12. After that certain amount of DI water was added until each

tube contained 30 mL solution. Therefore, the concentration of the final monomer solution was 2.5 mol/L (AM:AA = 4:1) with 1.5 wt% of initiator KPS and 2 wt% crosslinker MBA. Finally, 5 mL monomer solutions were transferred into beakers respectively and polymerized on the hot plate at 70°C for 10 min. The polymerized gel was cut into cubes and dried in oven at 60°C overnight for future the test. To test the water absorbency of beads with different crosslinking degrees, completely dried cubes were soaked in DI water at ambient conditions for 1 hour. Completely dried cubes were soaked in DI water at ambient conditions for 1 hour.

3.4 Synthesis of SAP Beads with Different Diameters

Previously, the diameter of the bead was controlled by the inner diameter of the silicone tube, which was both 1/16 inch (~1.58 mm). The diameter of dry beads was more than 1 mm. It took about 10 min for the bead to reach its equilibrium in water, which was not desirable for future applications [6]. Therefore, smaller beads are needed to achieve higher swelling rate and faster filtration. To achieve the goal, different glass tubes from 2 vendors were used. Detailed information is shown in the Table 1.

Table 1 - Inner and outer diameters information for glass tubes from different vendors.

No.	Inner Diameter (ID)	Outer Diameter (OD)	Vendor
1	1.5 mm	5 mm	GaTech Glass Shop
2	0.8 mm	3 mm	GaTech Glass Shop
3	0.5 mm	3 mm	F&D, inc
4	0.3 mm	3 mm	F&D, inc

Since glass tubes were used, commercial T junctions were no longer fit for the experiment. Therefore, 3D printing was used to create customized T junctions for the experiment. The design and finished product of T junction are shown in Figure 5. Detailed information is shown in the Table 2.

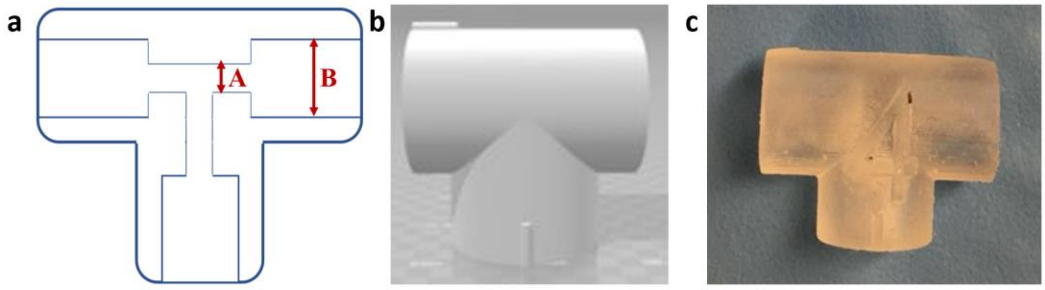

Figure 5 - T junctions. (a) Design of T junctions. (b) Solidworks image of a T junction. (c) final product of a T junction.

Table 2 - Dimensions information for different T junctions.

No.	Thru-hole dimension (A)	Connection dimension (B)
1	1.5 mm	5.2 mm
2	0.8 mm	3.2 mm
3	0.5 mm	3.2 mm
4	0.3 mm	3.2 mm

Because of the limitation of drilling the hole through the T junction and the difficulty of buying glass tube with thinner inner diameter, to reduce the size of beads using this method is not feasible. Inverse suspension polymerization is suited when the final polymer should be in the form of small beads with diameters less than 200 μm [28]. The actual bead size distribution is dependent on the balance between droplet break-up and droplet coalescence [29]. Therefore, small amounts of stabilizer are usually required to control the drop size

and the drop stability. The physical conditions also affect the droplet size distribution significantly by frictional forces and inertial forces, indicating that the impeller type or diameter and the agitation speed should be considered.

A curtained amount of distilled AA was neutralized by NaOH solution drop-by-drop until the pH reached 7 under ice water. Then a mixture of monomers, crosslinker MBA and initiator KPS in DI water was prepared. Stabilizers Span 80 (4 g/L) and Tween 60 (2 g/L) were dissolved in light mineral oil. The aqueous solution was introduced into the organic phase by syringe pumps and stirred at 85°C for 2 h [30]. Then, the suspension solution was introduced into methanol to precipitate the polymer. After drying precipitate in oven at 60°C overnight, the polymer powder was obtained.

3.5 Characterization of SAP Beads

3.5.1 Microscopy Images

The surface morphologies of the SAP beads were examined by two different scanning electron microscopes (Hitachi SU8010 and Zeiss Ultra60 FE SEM). Before SEM observation, all samples were dry and fixed on aluminium stubs.

3.5.2 Swelling Behaviors

Certain amounts of SAP beads synthesized with different compositions were soaked in DI water and allowed to swell. Samples were taken out from water after certain periods. Random beads are chosen as representatives to measure the diameter changes. After the surface water was removed carefully by tissue paper, the weight of the bead was measured

by an analytic balance. Equilibrium swelling was reached when the change of weight was negligible.

To study the effect of ionic strength of solution on swelling behaviors of SAP beads, certain amounts of sample SAP beads were soaked in NaCl solutions with various concentration and allowed to swell. Using the same procedure, the water absorbency at a certain given time for each sample was determined.

3.5.3 Reusability

The water absorbency of each sample at equilibrium was determined by the same procedure above. Then, samples were placed in the oven at 60°C overnight. After drying, samples were soaked in DI water and the water absorbency for each sample at equilibrium was measured again. The reusability of beads for different samples were determined.

3.6 SAP Beads for Concentrating *E. coli* in Water

The *E. coli* stock was prepared by incubating in 40 mL LB broth media at 37°C for 16-18 hours. Then the bacteria culture was mixed thoroughly by vortex. *E. coli* cells were harvested by centrifuging 1 mL of *E. coli* stock at 4000 rpm for 5 min and washed with DI water for three times. A 10 mL water sample containing certain amounts of *E. coli* was prepared. The initial *E. coli* concentration was ranged from 1×10^2 to 1×10^4 CFU/mL. Because plate-culturing method was used to determine the *E. coli* concentration, the result will not be reliable when the initial concentration is lower than 1×10^2 CFU/mL. In this experiment, 0.3 mm SAP beads with a water absorbency around 500 were used. Certain amounts of SAP beads (~0.02 g) were added to the water sample. After 5 min, remaining

water sample was transferred into another centrifuge tube with pipette and the remaining volume was measured. Because dried beads cohered to each other and formed clusters, it took time for them to swell and separate. Meanwhile, 200 μL sample was taken out for concentration measurement. These steps were repeated to concentrate the water sample to 1 mL. The *E. coli* concentration was measured by standard spread plating technique with six replicates for each measurement.

3.7 SAP Beads for Harvesting Algae in Water

Here 0.3 mm SAP beads with a water absorbency around 500 were applied to concentrate microalgae from culture suspension. *Chlorella kessleri* were grown in BG-11 medium containing the following chemicals: $NaNO_3$ (17.7 mM), KH_2PO_4 (0.18 mM), $MgSO_4 \cdot 7H_2O$ (0.30 mM), $CaCl_2 \cdot 2H_2O$ (0.25 mM), citric acid (0.03 mM), ferric ammonium citrate (0.03 mM), EDTA disodium salt dehydrate (0.003 mM), Na_2CO_3 (0.19 mM), H_3BO_3 (46 μM), $CuSO_4 \cdot 5H_2O$ (0.17 μM), $MnCl_2 \cdot 4H_2O$ (9.2 μM), $ZnSO_4 \cdot 7H_2O$ (0.77 μM) and $Na_2MoO_4 \cdot 2H_2O$ (1.6 μM). The pH was adjusted to 7.0. The cultivation was in a cylindrical bottle containing 500 mL of medium with continuous illumination.

After 7 days of cultivation, the concentration of the algae suspension was measured. Four tubes with each containing 10 mL of microalgae suspension was centrifuged at 8000 rpm for 10 min and then washed twice with DI water. Then samples were dried in an oven at 85 °C to a constant weight. A 20 mL algae suspension sample was prepared. Certain amounts of SAP beads (~0.02 g) were added to the suspension for the microalgae harvesting experiment. After 10 min, remaining sample was transferred into another tube. Meanwhile, the amount of water weight removed by SAP beads was measure by an

analytical balance, and 3 mL of sample was taken out to measure the dry weight. These steps were repeated for 5 times.

CHAPTER 4. RESULTS AND DISCUSSIONS

4.1 Effect of Composition on the Water Absorbency of SAP Beads

4.1.1 Effect of Crosslinking Degree

The results of the swelling experiments demonstrate that the crosslinker content and the total concentration of monomers both significantly affect the swelling behavior of SAP beads. From Figure 6, it is clear that the water absorbency decreases with the increase of crosslinker content from 0.05 to 1.0 wt% in all three scenarios with different monomer ratios. This result of decreasing water absorbency is attributed to the fact that crosslinking degree of the SAP beads increases when the crosslinker (MBA) content increases, and the rigidity of the beads in the swollen state is enhanced [31,32]. Another interesting result shows an increase in the amount of water absorbency with the dilution of the monomer mixture. For example, the water absorbency increases from 128.9 to 253.6 when the total monomer concentration decreases from 3 to 2 mol/L although the relative amount of crosslinking agent is set at 1 wt% and the two SAP beads have the same chemical composition. It is explained that as the water content increases during polymerization, small amounts of crosslinking agents react into the same growing polymer chain and form a loop structure, leading to a less crosslinked polymer [33]. The cyclization mechanism is shown in Figure 7. It is noticeable that when the total concentration of monomers and the percentage of cross-linker are both at a low level, the mixture is unable to form solid beads, resulting in fewer points for all 2 mol/L scenarios in Figure 6 with dashed lines.

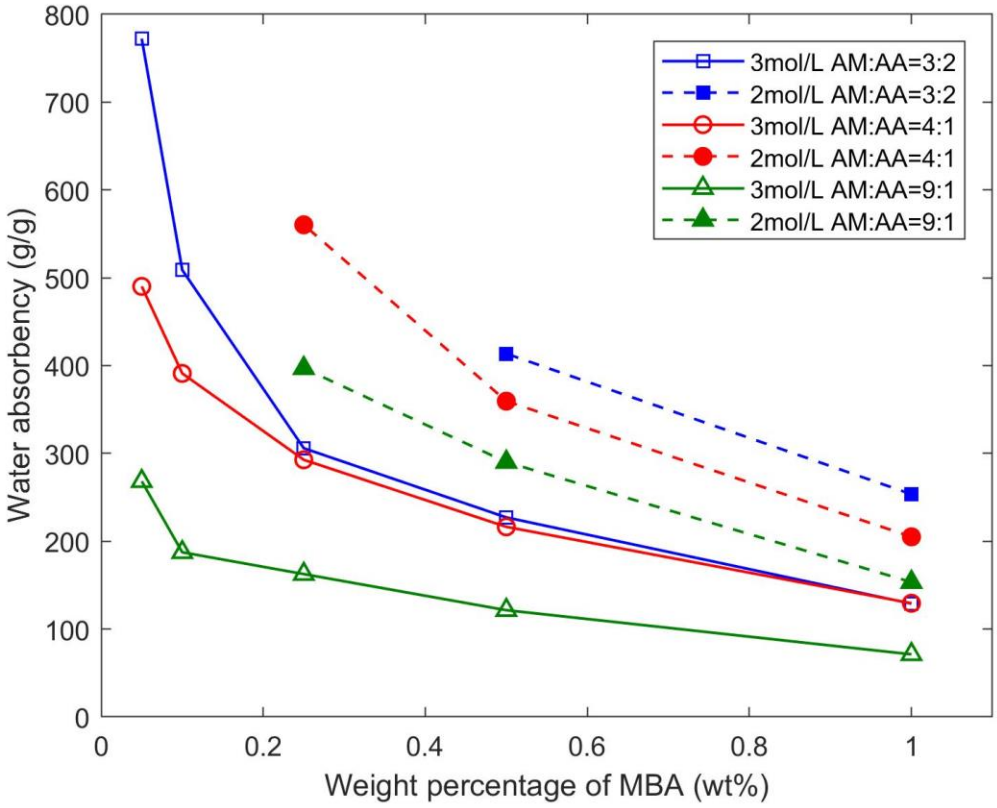

Figure 6 - Effect of crosslinking degree and dilution on water absorbency of the beads.

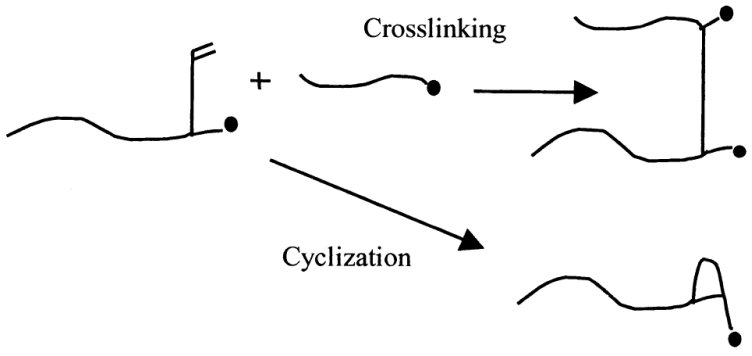

Figure 7 - Crosslinking and cyclization reactions. Adapted from "Structure and swelling of poly (acrylic acid) hydrogels: effect of pH, ionic strength, and dilution on the crosslinked polymer structure," by Jeannine E. Elliott, Mara Macdonald, Jun Nie, Christophern. Bowman, 2004, *Polymer*, 45, 1503-1510.

4.1.2 Effect of AA to AM Ratio

According to the plotted curve (Figure 8), the observed increase in water uptake capability with the increase in the AA monomer content should be attributed to the increase of -COO^- groups [34], which enhances the relaxation of polymer chains and increases the osmotic swelling pressure. However, we have noticed that if the content of AA is too high, the SAP beads may not be able to separate from each other after the two-step polymerization reaction because they are too stick or they may not be able to maintain its integrity when they swell.

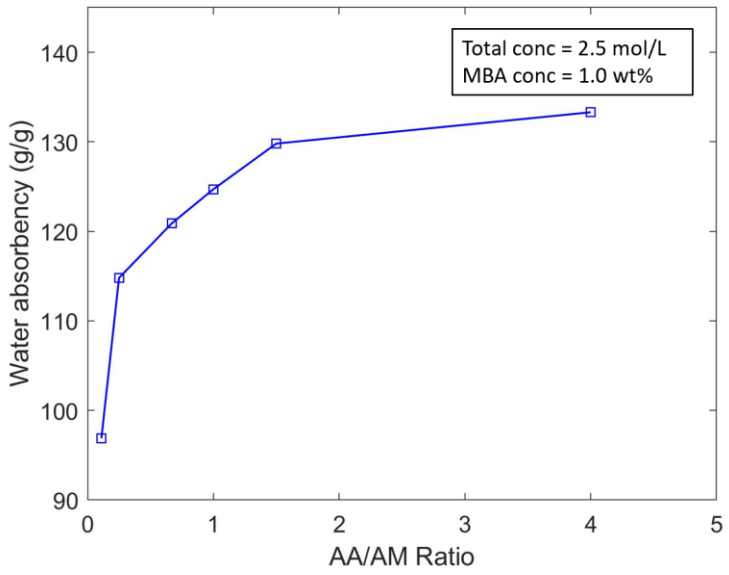

Figure 8 - Effect of monomer AA/AM ratio on the absorbency of SAP beads.

4.1.3 Effect of pH

The water absorbency of the SAP beads prepared from monomer solutions with various pH values is shown in Figure 9. When the mixture is neutralized to pH = 7, the SAP beads show the highest water absorption capacity.

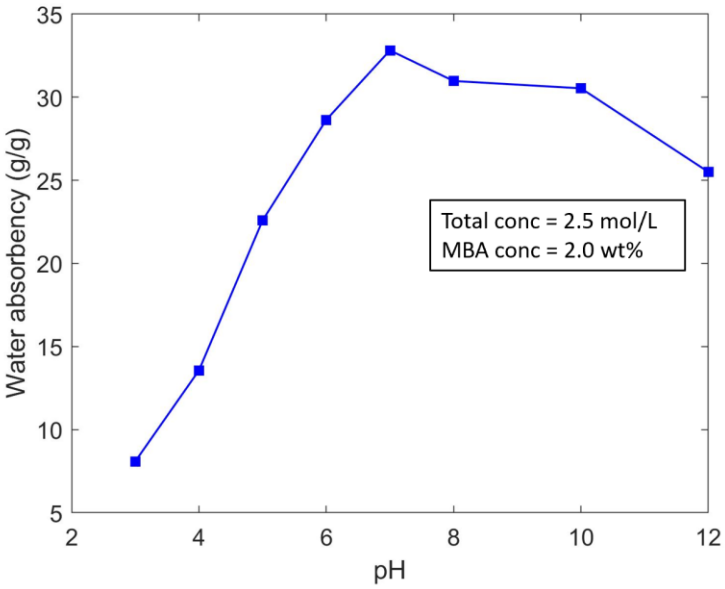

Figure 9 - Effect of pH on beads swelling behavior.

From the plot, the water absorbency increases from pH 3-7, the observed increase in the equilibrium water uptake with the increase of the degree of neutralization should be attributed to the fact that as the degree of neutralization increases, the number of $-COO^-$ group also increases. Because of the repulsion among similarly charged $-COO^-$ groups, the chain relaxation is enhanced [35]. Moreover, the concentration of counter ions (Na^+) also increases, leading to a higher osmotic swelling pressure.

However, water absorbency decreases slightly from pH 7-12, where the whole system is basic. The redundant free counter ions (Na^+) condense on the polymer chain, which indicates the number of free ions decreases, leading to a decrease in osmotic pressure [36, 37]. This synergy between sodium carboxylate and carboxylic acid groups with an 85% of neutralization produces the highest water absorbency.

4.2 Products of SAP Beads with Different Sizes and Compositions

Table 3 below shows the dry bead sizes produced by different glass tubes and the inverse suspension polymerization method. During the solution polymerization experiments, using the glass tube with 0.3 mm ID was unable to produce SAP beads.

Poiseuille Equation explains that the pressure needed for a fluid maintaining a certain flow rate increases with the decrease of pipe diameter.

$$\Delta P = \frac{128\mu LQ}{\pi D^4}$$

where D is the pipe diameter, L is the length of pipe, μ is the viscosity of the fluid, and Q is the volumetric flow rate. The connection between the T junction and the glass tube is not secure enough to withstand such high pressure, which triggers the leak of streams from the connection point.

Table 3 - Dry bead sizes produced by glass tubes with different inner diameters.

Glass tube ID	Dry beads diameter
1.5 mm	~1 mm
0.8 mm	~ 0.5 mm
0.5 mm	~ 0.3 mm
0.3 mm	N/A
Inverse suspension	Varied size (20-100 μm)

Figures 10a, d, g, and j below are photos taken by digital microscope. Among them a, d, and g show the dry beads synthesized using different types of glass tubes respectively, and

j shows beads synthesized by the inverse suspension polymerization method. Figures 10b, e, h, and k were taken by Microscope, the average dry bead sizes are around 1.0 mm, 0.5 mm, and 0.3 mm, respectively. The dry bead sizes polymerized by inverse suspension method are randomly distributed from 20 μm to 100 μm. For example, the diameter of beads in Figure 10k is 70 μm. It is difficult to acquire beads with an uniform size using inverse suspension polymerization method since the diameter is determined by several synthetic conditions such as the speed of agitator, the concentration of stabilizer [38-41]. Figure 11 shows the diameter distribution of beads synthesized via the inverse suspension polymerization. More than 200 beads has been counted and the average size is 52 (±30.3) μm. Figures 10c, f, i, and l are pictures showing different sized beads after swelling in DI water, respectively. The color of beads are blue in Figure 10l because a food dye has been added to the monomer solution.

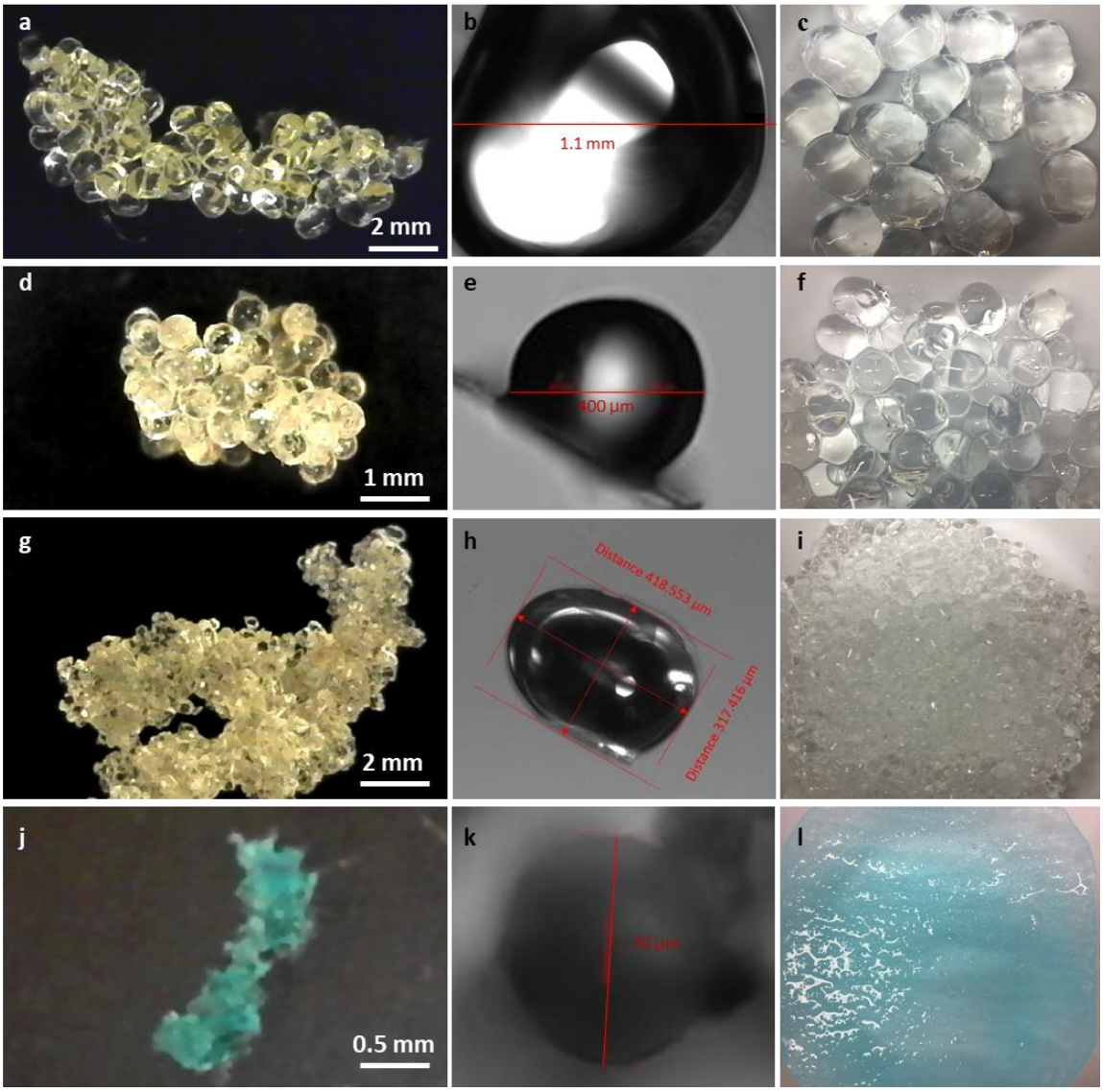

Figure 10 - Images of SAP beads with different sizes. (a-c) SAP beads prepared by ID 1.5 mm glass tube; (d-f) SAP beads prepared by ID 0.8 mm glass tube; (g-i) SAP beads prepared by ID 0.5 mm glass tube; and (j-l) SAP beads prepared by inverse suspension polymerization. The left column, middle column, and right column of the images were taken by Digital View, a Zeiss advanced microscope, and iphone, respectively.

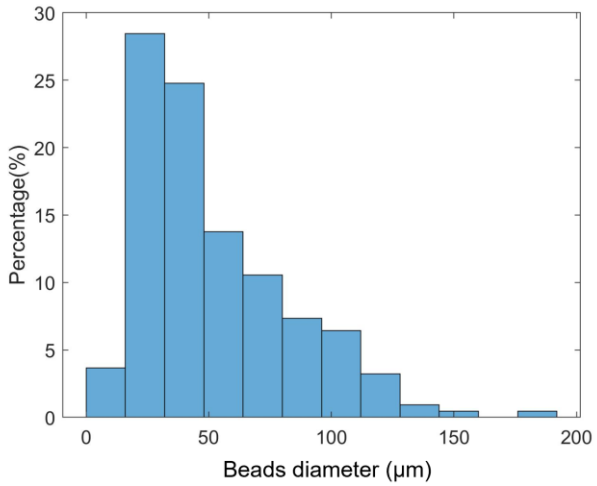

Figure 11 - Size distribution of SAP beads synthesized by inverse suspension polymerization.

After the study of composition and production of beads with 3 different sizes, 9 types of beads were fabricated and the relevant parameters are given in Table 4.

Table 4 - Products of beads with different diameters and compositions.

No.	Diameter (mm)	Total conc (mol/L)	AA:AM Ratio	KPS (wt%)	MBA (wt%)	Water absorbency (g/g)
1	0.3	5	3:2	1.2	1	~100
2		4	3:2	1.2	0.5	~300
3		4	3:2	1.2	0.25	~500
4	0.5	5	3:2	1.2	1	~100
5		4	3:2	1.2	0.5	~300
6		4	3:2	1.2	0.25	~500
7	1.0	5	3:2	1.2	1	~100
8		4	3:2	1.2	0.5	~300
9		4	3:2	1.2	0.25	~500

4.3 Properties of the SAP Beads

4.3.1 Surface Morphology

SEM micrographs of SAP beads taken by Hitachi SU8010 are shown in Figure 12. Before the SEM observation, these beads were coated with gold particles. These samples present a coarse surface with some wrinkles. We were not able to visualize the water channels in SAP beads.

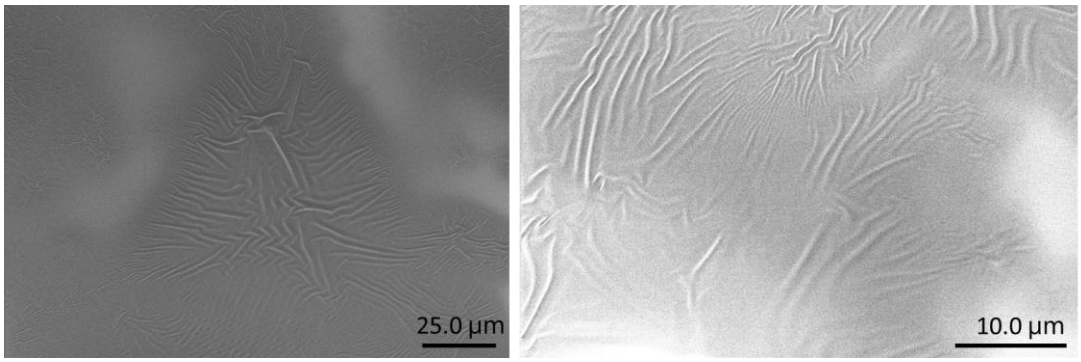

Figure 12 - Scanning electron microscope (SEM) images of the outer surface of beads taken by Hitachi SU8010.

Figure 13 shows the dry beads without coating characterized by Zeiss Ultra60 FE-SEM. The images show obvious charging effect [42]. Static electric charges on the specimen surface were accumulated, which influences the electron signals and deteriorates the image information.

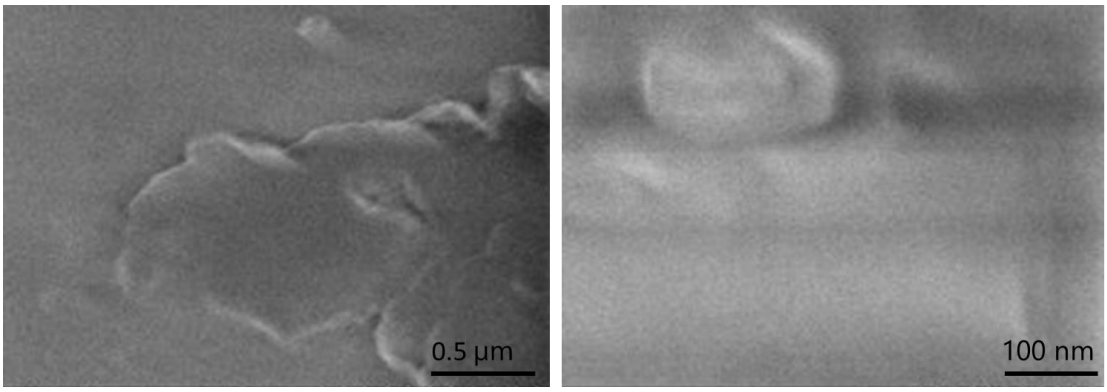

Figure 13 - Scanning electron microscope (SEM) images of the outer surface of beads taken by Zeiss Ultra60 FE-SEM.

4.3.2 Sweling Behaviors

The diameter changes of beads with different sizes were measured when soaking in deionized water, shown in Figure 14. From Figure 14a, the diameter of beads increases gradually from 0.3 mm and reaches ~7.5 fold of its original value within 5 minutes. Expectedly, it takes much longer for beads with larger initial sizes to reach equilibrium, such as 40 minutes for beads with initial diameter of 0.5 mm to reach 3.8 mm (Figure 14b) and almost 2 hours for beads with initial diameter of 1 mm to reach 7.3 mm (Figure 14c). The diameter changes of beads synthesized by inverse suspension polymerization when soaking in water are not able to be measured with this method, because the swelling rate is so fast when the bead size is smaller than 100 µm that they reach their maximum capacity in seconds.

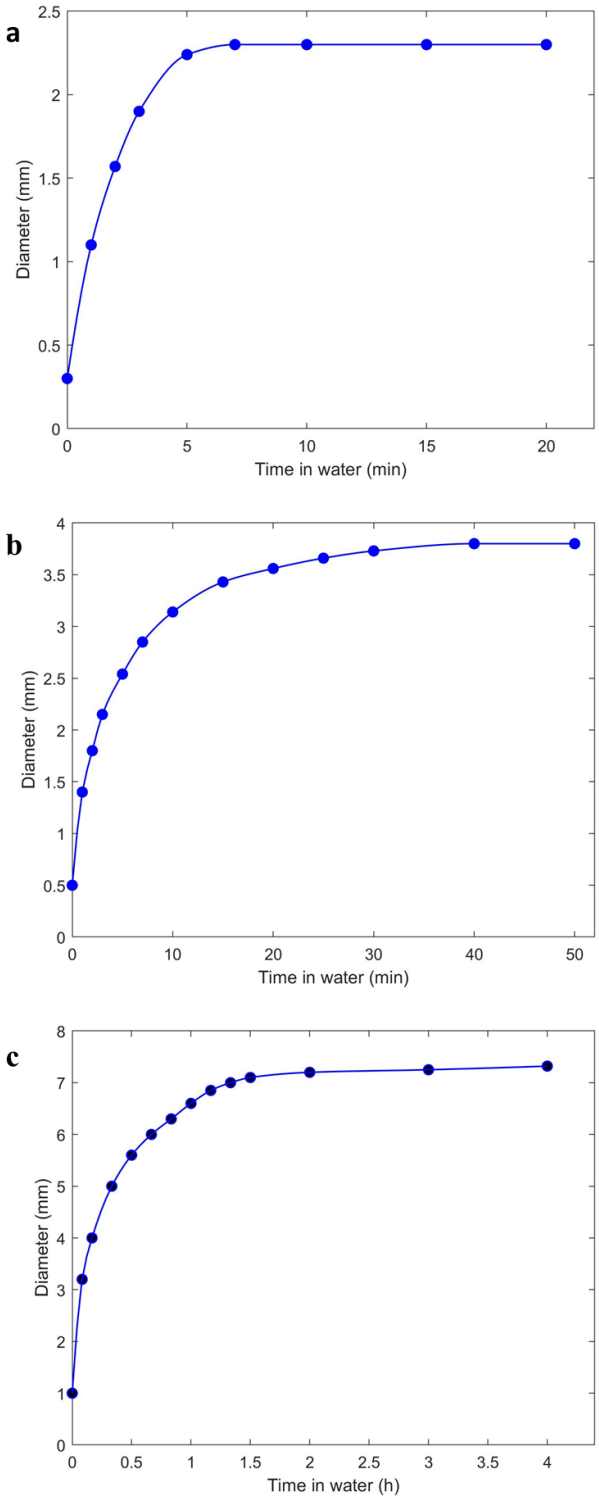

Figure 14 - Size change of the SAP beads when soaking in DI water. (a) Beads with a 0.3 mm dry diameter. (b) Beads with a 0.5 mm dry diameter. (c) Beads with a 1 mm dry diameter.

The swelling and diffusion characteristics were investigated by a kinetic analysis. The normalized degree of swelling Q_t was calculated as:

$$Q_t = \frac{M_s - M_0}{M_0} = \frac{M_t}{M_0}$$

where M_s represents the total mass at time *t*, M_0 is the mass of dry beads, M_t means the water absorbed by the SAP beads.

Similarly, the normalized degree of swelling at equilibrium Q_e was calculated as:

$$Q_e = \frac{M_\infty - M_0}{M_0} = \frac{M_e}{M_0}$$

where M_∞ and M_e represent the total mass of SAP beads and the mass of water absorbed by SAP beads at equilibrium respectively.

The kinetic mechanism was analyzed by a first-order swelling kinetic model. This model assumes the absorption rate depends on the quantity of unoccupied sites [43]. The mathematical equation is expressed:

$$\frac{Q_t}{Q_e} = 1 - e^{-kt}$$

Another form of expression is:

$$\ln\left(\frac{Q_e - Q_t}{Q_e}\right) = -kt$$

where k is the equilibrium swelling rate constant.

Figure 15a illustrates the diameter changes of SAP beads with different dry diameters and Figure 15b shows the first order swelling kinetics. It is clear that equilibrium is attained at a faster rate by smaller beads.

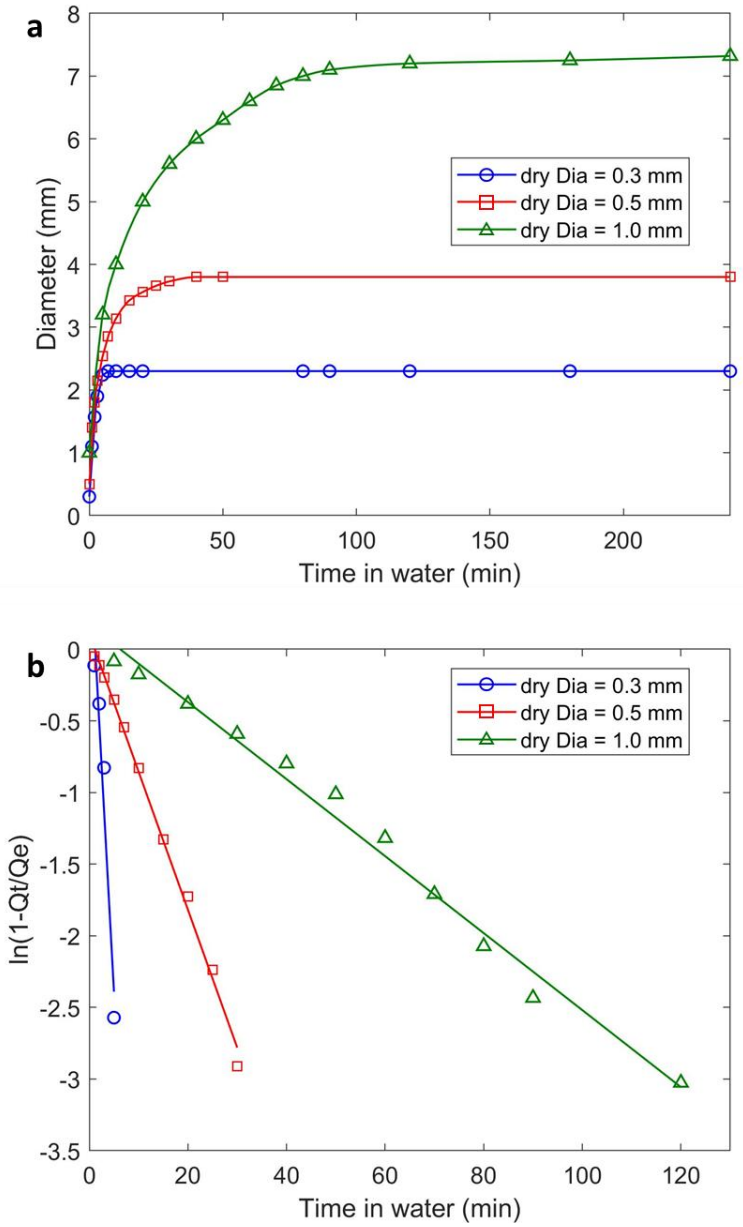

Figure 15 - Swelling behavior comparison between SAP beads with different sizes. (a) Dependency of size change on time for beads with different diameters. (b) First-order swelling kinetics for beads.

Swelling plots and its corresponding swelling rate constant for each type of bead are shown in Figure 16. The calculated rate constants are given in Table 5. From Figures 16a, c, and e, it is clear that though equilibrium water absorbency is higher for the less crosslinked systems, it takes less time to reach equilibrium by more crosslinked systems.

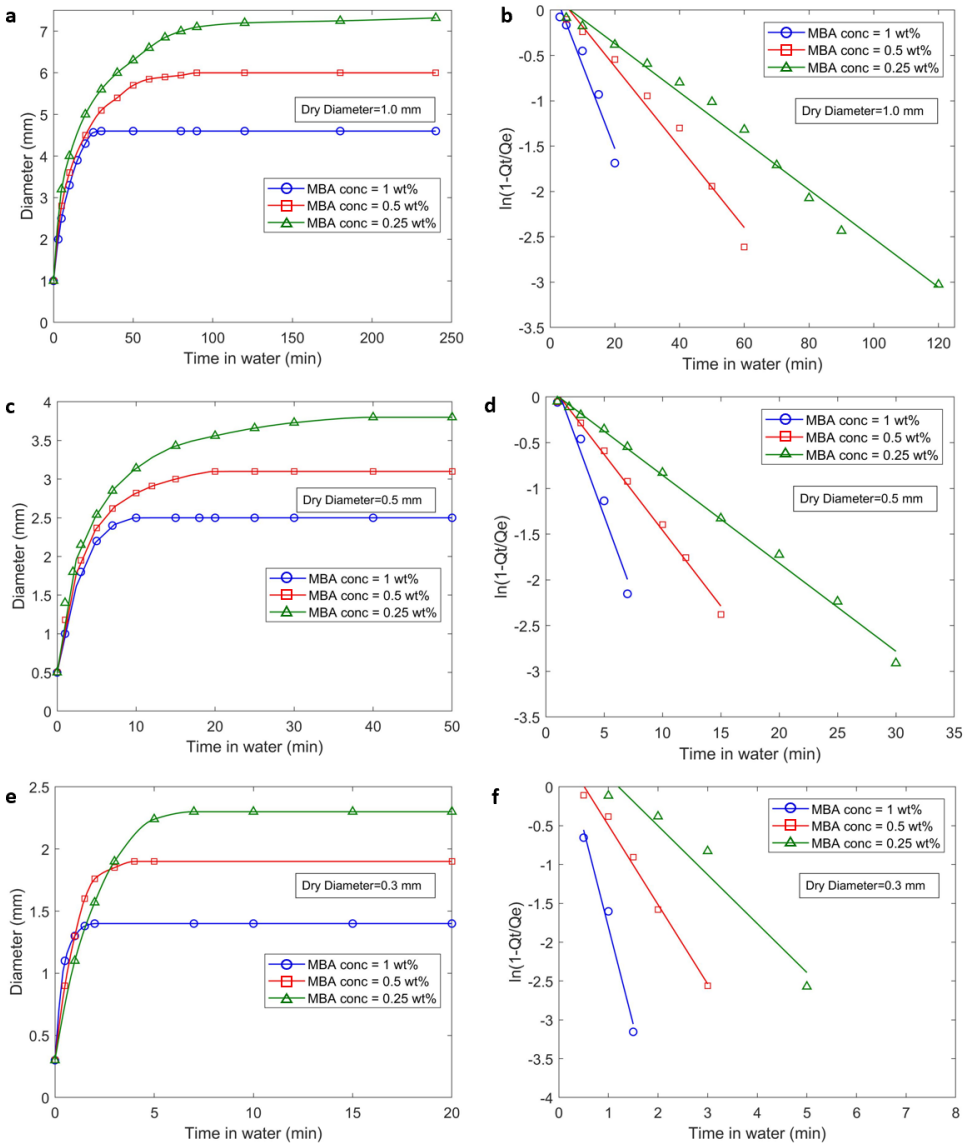

Figure 16 - Swelling behavior comparison between SAP beads with different crosslinking degrees. (a), (c), and (e) Dependency of size change on time for beads with 1.0 mm, 0.5 mm, and 0.3 mm diameter and different crosslinking degrees. (b), (d), and (f) Corresponding first-order swelling kinetics for different beads.

Table 5 - Production of nine types of beads with different diameters and water absorbency.

No.	Dry beads diameter (mm)	Beads diameter at equilibrium (mm)	Water absorbency (g/g beads)	Swelling rate constant k (min^{-1})
1	0.3	1.4	101	2.5005
2		1.9	311	1.0213
3		2.3	450	0.6296
4	0.5	2.5	125	0.3480
5		3.1	297	0.1658
6		3.8	466	0.0963
7	1.0	4.6	112	0.0922
8		6.0	308	0.0444
9		7.4	437	0.0269

According to Table 5, the swelling rate constant increases as the crosslinking degree increases for beads with the same size, and as the beads have larger sizes when the crosslinking degree is the same.

4.3.3 Water Absorbency under Different Ionic Strengths

The water absorbency of SAP beads in saline solutions are important since in a lot of applications, such as agriculture, SAP beads need to interact with liquid containing salts. The influence of ionic strength on the water absorbency of SAP beads were tested. Generally speaking, the water absorbency decreases with the increase of ionic strength in NaCl solution compared with that in DI water (Table 6). When the ionic strength is higher, the ionic concentration gradient is decreased, which means that the ionic osmotic pressure

between the external solution and the SAP beads decreases, result in the decline of water absorbency [43, 44]. According to the result from Figure 17a, 0.3 mm beads have water absorbency of 433 in DI water, whereas they only absorb 141 times its weight of in a NaCl solution with an ionic strength of 0.017 mol/L. Similar trend is also shown for all beads with different crosslinking degrees in Figure 17b while the trend is more significant for beads that have higher water absorbencies originally. For example, the water absorbency decreases from 433 to 50 for beads with 0.25 wt% of crosslinker, meanwhile, the water absorbency decreases from 125 to 38 for beads 1.0 wt% of crosslinker.

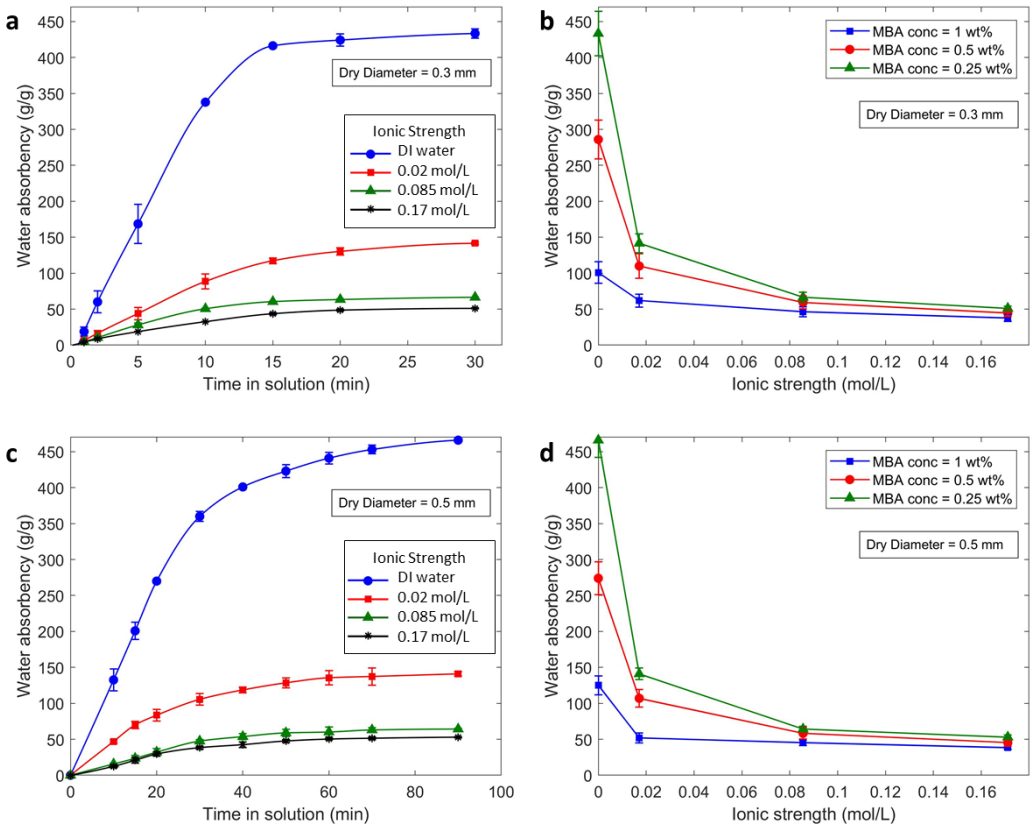

Figure 17 - Effect of ionic strength of solution on the water absorbency of SAP beads. (a) and (c) Dependency of water absorbency on time for beads with 0.3 mm, 0.5 mm diameter respectively and 0.25 wt% of crosslinker in NaCl solutions with different concentrations. (b) and (d) Dependency of water absorbency on solution ionic strength for beads with 0.3 mm, 0.5 mm diameter respectively and different crosslinking degree.

The reason for taking almost half an hour to reach the equilibrium is that dry beads stick with others and form a cluster that is difficult to separate. When a whole cluster is submerged in water, it takes much longer for inner beads to access water. Therefore, Figure 17 only shows the water absorbency capacity of beads in salt solution without showing the real swelling behavior of beads. One bead with a diameter of 0.3 mm was immersed in 10 g/L NaCl solution to test the real swelling behavior under the microscope. Figure 18 shows the diameter change curve. According to the curve, the bead swells fast in the first 30 seconds. After 5 min, the diameter changes slowly, which is consistent with the time interval needed in DI water. The curve is not smooth because the swelling kinetics in different states are different.

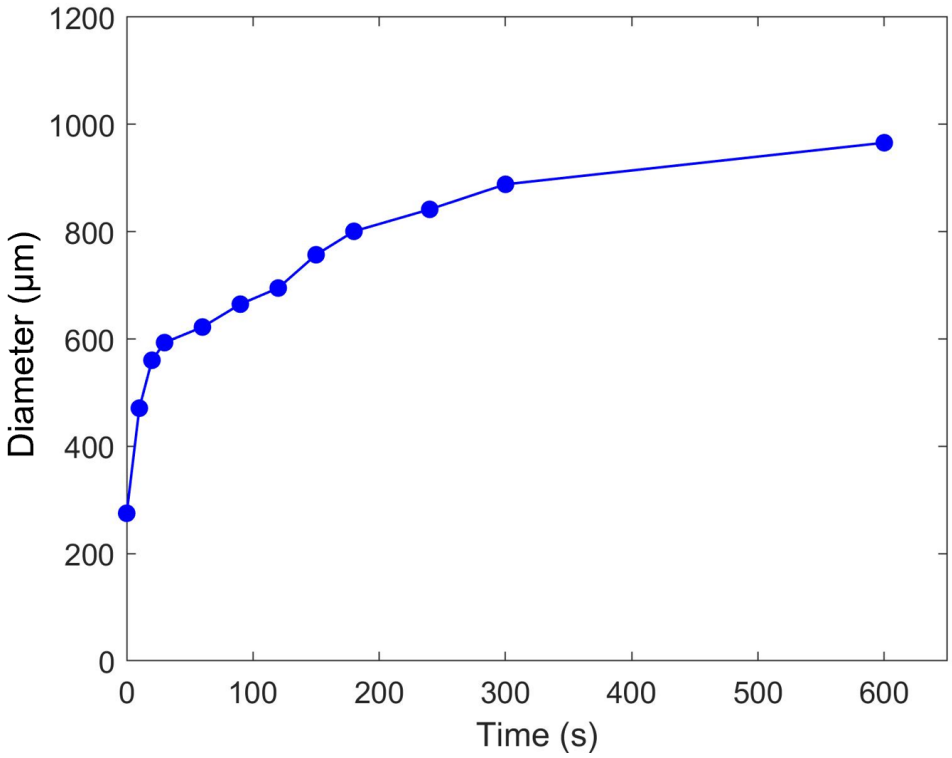

Figure 18 – Swelling behavior of 0.3 mm SAP beads in 10 g/L NaCl solution.

Table 6 - Water absorbency for SAP beads with different crosslinking degree in deionized and saline water.

Dry beads diameter (mm)	Crosslinker weight percentage (wt%)	Water Absorbency (g/g)			
		Ionic strength (mol/L)			
		0	0.02	0.085	0.17
0.5	1.0	125	52	45.3	38.3
	0.5	274	107	58.3	45.4
	0.25	466	141	64.2	53
0.3	1.0	101	62	46.5	37.8
	0.5	286	110	60	45
	0.25	433	141	66.5	51

4.3.4 Reusability

Reusabilty of beads is also another important character because beads with higher reusability can be recycled more times, which reduce the overall cost and are more environmental friendly. Figures 19a and b show the water absorbency changes with the increasing number of uses. There is a general trend that water absorbency decreases when they are recycled, while no siginificant difference between beads with various sizes. However, accroding to the calculated decreasing rate from Table 7, if we assume it decreases linearly, the water absorbency decreases slightly faster for beads with lower corsslinking degree. The percentage of capacity loss is between 20 – 40%.

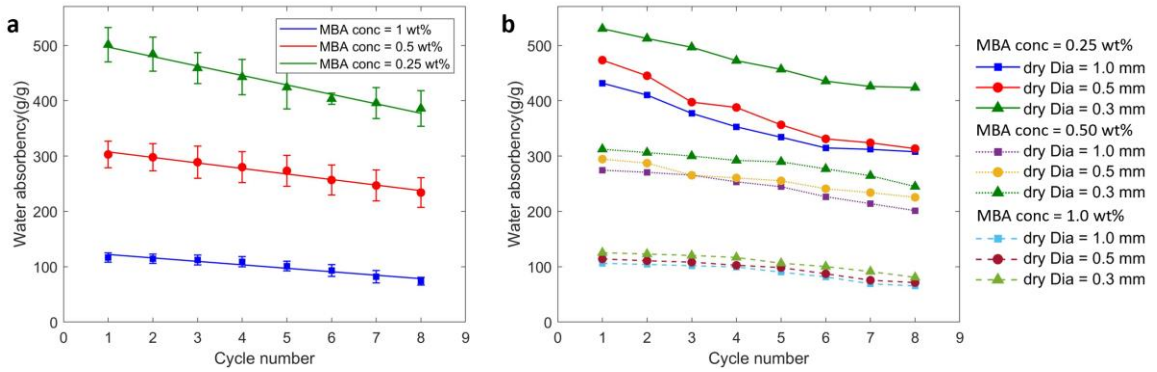

Figure 19 - Reusability of SAP beads. (a) Water absorbency of beads when recycled with different crosslinking degrees. (b) Water absorbency of beads when recycled with different sizes.

Table 7 - Dependency of water absorbency decreasing rate for beads on diameters.

Water absorbency (g/g)	Water absorbency decreasing rate	Percentage of loss
~100	6.25	36%
~300	10.01	23%
~500	17.07	23%

4.4 *E. coli* Concentrating

Waterborne pathogenic microorganisms have been a serious threat to public health and safety for decades. However, the detection of bacterial contamination with low concentration or large volume is still limited [45, 46]. Therefore, SAP beads were applied to concentrate water sample containing *E. coli*. Because the size of *E. coli* is around 0.5 μm in width by 2 μm in length, they are excluded in residual.

Results were shown in Figures 20 a-c. It is obvious that the *E. coli* concentration increases gradually with the decrease of water volume. The dashed lines represent the theoretical *E. coli* concentration calculated using the assumption that there is no loss of *E. coli* during the concentrating procedure. The measured concentrations do not have a significant difference with the theoretical concentration, indicating the concentrating method is feasible and efficient. The recovery efficiencies are defined by following equations:

recover efficiency for each step: $\eta_i = (V_i \times C_i)/(V_{i-1} \times C_{i-1})$, where i = 1-5;

average recover efficiency for each test: $\eta_{avg} = (\eta_1 + \eta_2 + \eta_3 + \eta_4 + \eta_5)/5$;

cumulative recovery efficiency for each test: $\eta_{cum} = \eta_1 \times \eta_2 \times \eta_3 \times \eta_4 \times \eta_5$.

Table 8 summarizes the recovery efficiencies of the 5 concentrating steps of three experiments with different initial *E. coli* concentrations. There is a general trend that the recovery efficiency decreases as the concentration of *E. coli* becomes higher. As shown in Figure 20d, the average recovery efficiency and the cumulative recovery efficiency both decrease from 99.35% to 95.75% and 95.79% to 80.17% respectively. It also can be observed by the 5th step in each test, where the recovery efficiency is lower compared with the first four steps.

For each concentrating step, if the amount of SAP beads added to the water sample is too low, it takes longer time or more steps to concentrate from 10 mL to 1 mL. Oppositely, if the amount of SAP beads added in each step is too high, the SAP beads take up most of the water and are not able to suspend in water sample, which may diminish the recovery efficiency. Therefore, the concentration degree is defined by the ratio of the sample volume

before and after one step: $\text{Degree} = V_i/V_{i-1}$. The effect of concentration degree was studied by adding different amount of SAP beads to 10 mL of water sample for one single step (Figure 21). When the concentration degree is ~2, which means that 10 mL of water sample is concentrated to ~5 mL, the recovery efficiency is around 90%. As the concentration degree increases, the recovery efficiency drops proportionally. The recovery efficiency is only 63% when the concentration degree is 7.7.

The results of these two experiments might be explained by the microbial adhesion onto the surface of SAP beads. Both situations, where the *E. coli* concentration is high, or the number of beads is large, indicate a poor mixing condition that at certain part in the water sample there might not be enough water for beads to swell and result in the adhesion of *E. coli* onto the SAP beads.

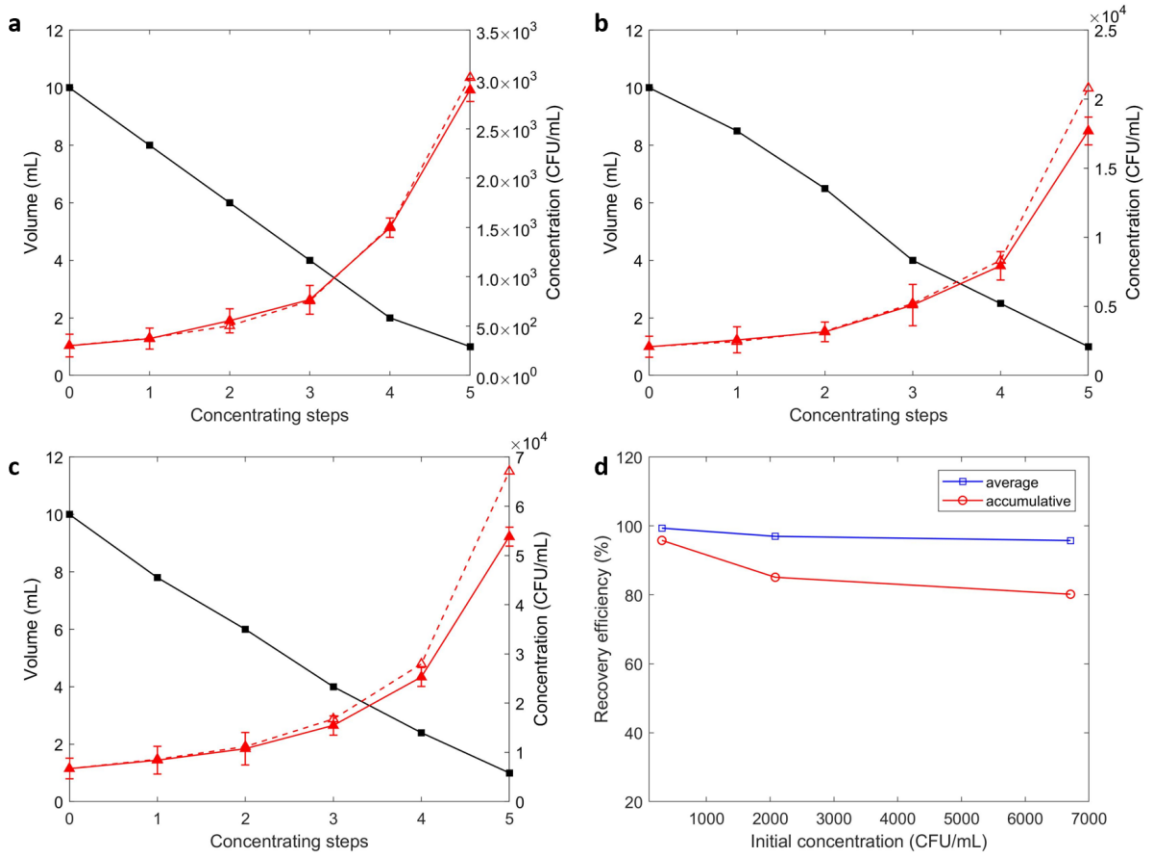

Figure 20 - Performance of applying SAP beads to concentrate *E. coli* microorganisms. (a), (b) and (c) in different initial concentrations: 3.0×10^2 CFU/mL, 2.1×10^3 CFU/mL, and 6.7×10^3 CFU/mL respectively. (d) Summary of the average and cumulative recovery efficiencies for the three concentrations tests.

Table 8 - Summary of the average and cumulative recovery efficiencies for the three concentrations tests.

Initial Concentration (CFU/mL)	Concentrating Steps					Average	Cumulative
	1	2	3	4	5		
3.0×10^2	98.54	111.69	92.18	97.72	96.62	99.35	95.79
2.1×10^3	105.02	93.73	99.63	97.18	89.28	96.97	85.10
6.7×10^3	97.99	98.18	95.85	98.16	88.56	95.75	80.18

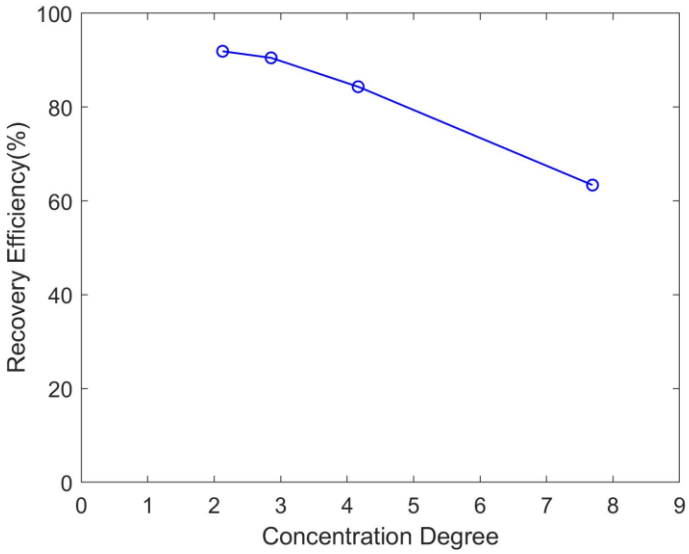

Figure 21 - Recovery efficiencies of a single concentrating step with different concentration degrees.

4.5 Algae Harvesting

Microalgae harvesting has become the main constriction of the microalgae commercialization process since traditional harvesting methods, such as centrifugation, filtration, and flotation are very energy consuming [47, 48].

The experimental result in Figure 22a shows that the algae concentration increased from 2.03 g/L to 2.35 g/L in 1 hour. The dashed line represents the theoretical algae concentration and the solid red line represents the measured algae concentration. During the harvesting process, the volume of solution merely decreased about 5 mL. In each step, the water absorbency of beads decreased from 54.67 g/g to 34.7 g/g. This low water absorbency is mainly attributed to the high ionic strength of the medium, which has a dramatic negative impact on the performance of SAP beads. The short time interval for each step might also offset the capacity of SAP beads. Since beads are not reused after one harvesting step, dry beads need time to swell and separate from each other. For future

experiment, it is more practical to add more beads in each step and make beads less aggregated.

Another observation is that the recovery efficiency gradually decreased step by step from 99.37% to 93.14%. Although used SAP beads become green when they were separated from solution, the high recovery efficiency indicates this harvesting method is still applicable and reliable. The accumulative recovery efficiency for 5 steps is 85.96%.

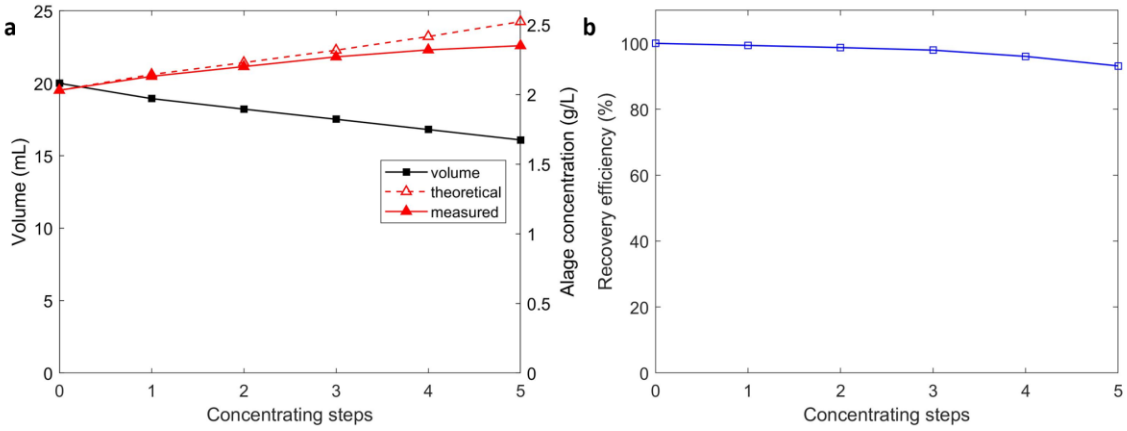

Figure 22 - Performance of applying SAP beads to harvest microalgae in solution. (a) Comparison between measured and theoretical concentrations of algae in each step. (b) Recovery efficiency decreases in each step.

CHAPTER 5. CONCLUSIONS

This research project used a simple two-step method to synthesize poly (acrylamide-co-acrylic acid) (P(AM-co-AA)) SAP beads. In this method, monomer solutions and carrier phase (silicone oil) were injected to glass tube. Then small droplets were formed at the T junction and pre-polymerized under heat. These partially polymerized polymer beads were further healed in the carrier phase under certain temperature. Compared with previous method, the stability of the synthetic system of the new two-step polymerization method is largely improved.

A thorough study on the compositions of SAP beads was conducted. According to the experiment results, the water absorbency of SAP beads is affected by the crosslinking degree, the total concentration of monomer solution, the monomer ratio, and the pH value of the monomer solution. To a certain point, higher water absorbency can be expected when the crosslinking degree is low, the monomer solution is diluted, the content of acrylic acid (AA) is high, and the solution is partially neutralized.

By changing the inner diameter of the glass tube, beads is obtained with three different sizes: 0.3 mm, 0.5 mm, and 1.0 mm. Inverse suspension polymerization can be used to produce beads under 100 μm, although the size distribution is hard to control.

Nine types of beads are obtained which are classified according to their sizes and water absorbencies ranged around 100, 300, and 500. Since SAP beads are produced by batch, it is not applicable to maintain the water absorbency at an exact value every time.

From the properties of SAP beads studies, beads with smaller sizes reach their equilibrium in water at a faster rate than beads with larger sizes. Beads with higher crosslinking degrees show lower water absorbencies but have higher swelling rate constants. The water absorbency of SAP beads decreases dramatically when soaked in saline water. Meanwhile, beads with a high initially water absorbency are more vulnerable in saline environment. There is a general trend that water absorbency decreases when beads are recycled, but the decreasing rate is high for beads with an initial high absorbency.

We investigated two possible applications of SAP beads: *E. coli* concentration and algae harvesting. In our experiments, *E. coli* solution was concentrated from 10 mL to 1 mL by five steps in about 15 minutes with a relatively high recover efficiency. In the algae harvesting experiment, water absorbed by each step is limited because the medium contains salts.

REFERENCES

[1]. A.W. ZULARISAM, A.F. ISMAIL, RAZMAN SALIM., "Behaviours of natural organic matter in membrane filtration for surface water treatment – a review," Desalination., 194, 211-231, 2006.

[2]. F. L. HUA, Y. F. TSANG, S. N. SIN, et al., "Performance study of ceramic microfiltration membrane for oily wastewater treatment," Chemical Engineering Journal., 128, 169-175, 2007.

[3]. SUKHVINDER P. S. BADWAL, FABIO T. CIACCHI., "Ceramic membrane technologies for separation," Adv. Mater., 13, 993-996, 2001.

[4]. CRISTINA ALMANDOZ, CECILIA PAGLIERO, ARIEL OCHOA, JOSE MARCHESE., "Corn syrup clarification by microfiltration with ceramic membranes," Journal of Membrane Science., 363, 87-95, 2010.

[5]. WHITAKER, S. "Flow in porous media I: a theoretical derivation of Darcy's law," Transport in Porous Media., 1, 3-25, 1986.

[6]. XING XIE, JANINA BAHNEMANN, SIWEN WANG, YANG YANG, MICHAEL R. HOFFMANN., "Nanofiltration enabled by superabsorbent polymer beads for concentrating microorganisms in water samples," Scientific Report., 6, 20516, 2016.

[7]. ENAS M. AHMED., "Hydrogel: Preparation, characterization, and applications: A review," Journal of Advanced Research., 6, 105-121, 2015.

[8]. K. KABIRI, H. OMIDIAN, M. J. ZOHURIAAN-MEHR, S. DOROUDIANI., “Superabsorbent hydrogel composites and nano composites: A review,” Polymer Composite., 32, 277-289, 2011.

[9]. BUCHHOLZ FL, PEPPAS NA., “Superabsorbent polymers science and technology,” ACS Symposium Series., 573, 1994.

[10]. QYRESEARCH GROUP., “Global superabsorbent polymer market research report,” 2018.

[11]. ECATERINA STELA DRAGAN., “Design and applications of interpenetrating polymer network hydrogels. A review,” Chemical Engineering Journal., 243, 572-590, 2014.

[12]. MOHAMMAD J. ZOHURIAAN-MEHR, KOUROSH KABIRI., “Superabsorbent polymer materials: A review,” Iranian Polymer Journal., 17, 451-477, 2008.

[13]. FATIMA ROSA, JOAO BORDADO, MIGUEL CASQUILHO., “Kinetics of water absorbency in AA/AMPS copolymers: applications of a diffusion-relaxation model,” Polymer., 43, 63-70, 2002.

[14]. A. DAS, V. K. KOTHARI, S. MAKHIJA, K. AVYAYA., “Development of high-absorbent light-weight sanitary napkin,” J Appl Polym Sci., 107, 1466-1470, 2008.

[15]. JUN CHEN, HAESUN PARK, KINAM PARK., “Synthesis of superporous hydrogels: hydrogels with swelling and superabsorbent properties,” J Biomed Mater Res., 44, 53-62, 1999.

[16]. JUN CHEN, KINAM PARK, et al., “Gastric retention properties of superporous hydrogel composites,” J Control Release., 64, 39-51, 2000.

[17]. M. BAKASS, A. MOKHLISSE, M. LALLEMANT., “Absorption and desorption of liquid water by a superabsorbent polymer: effect of polymer in the drying of soil and the quality of certain plants,” J Appl Polym Sci., 83, 234-243, 2002.

[18]. M. J. ZOHURIAAN-MEHR, H. OMIDIAN, S. DOROUDIANI, K. KABIRI., “Advances in non-hygienic applications of superabsorbent hydrogel materials,” J Mater Sci., 45, 5711-5735, 2010.

[19]. H. X. D. LEE, H. S. WONG, N.R. BUENFELD., “Self-sealing of cracks in concrete using superabsorbent polymers,” Cement and Concrete Research., 79, 194-208, 2016.

[20]. HANY EL-HAMSHARY., “Synthesis and water sorption studies of PH sensitive poly (acrylamide-co-itaconic acid) hydrogels,” European Polymer Journal., 43, 4830-4838, 2007.

[21]. SHIDAN CUMMINGS, YUJIE ZHANG, MARC A. DUBE et al., “Determination of reactivity ratios for the copolymerization of poly (acrylic acid-co-itaconic acid),” J APPL POLYM SCI., 133, 44014, 2016.

[22]. PENG LI, JING CHEN, JIN ZHU et al., “Itaconic acid as a green alternative to acrylic acid for producing a soybean oil-based thermoset: synthesis and properties,” ACS Sustainable Chem Eng., 5, 1228-1236, 2017.

[23]. G.R. MAHADAVINIA, M.J. ZOHURIAAN, et al., “Modified chitosan superabsorbent hydrogels from poly (acrylic acid-co-acrylamide) grafted chitosan with salt and PH responsiveness properties,” European Polymer Journal., 40, 1399-1407, 2004.

[24]. JUNPING ZHANG, QIN WANG, AIQIN WANG., “Synthesis and characterization of chitosan-g-poly (acrylic acid)/attapulgite superabsorbent composites,” Carbohydrate Polymers., 68, 367-374, 2007.

[25]. JESSICA X. H. WONG, HUAZHONG YU., “Preparation of transparent superhydrophobic glass slides: demonstration of surface chemistry characteristics,” Journal of Chemical Education., 90, 1203-1206, 2013.

[26]. BROOKS, B. W., “Suspension polymerization processes,” Chemical Engineering and Technology., 33, 1737-1744, 2010.

[27]. P. J. DOWDING, B. VINCENT., “Suspension polymerization to form polymer beads,” Colloids and Surfaces A: Physicochemical and Engineering Aspects., 161, 259-269, 2000.

[28]. JIANJUN XIE, HUIYING ZHANG, DELONG RAN., “Preparation and absorbencies of poly(acrylate-co-acrylamide) superabsorbent by inverse suspension polymerization,” Advanced Materials Research., 223, 1257-1261, 2011.

[29]. SAMANEH KHANLARI, MARC A. DUBE., “Effect of pH on poly (acrylic acid) solution polymerization,” Journal of Macromolecular Science, Part A: Pure and Applied Chemistry., 52, 587-592, 2015.

[30]. NIKOLAOS A. PEPPA, PAOLO COLOMBO., “Analysis of drug release behaviour from swellable polymer carriers using the dimensionality index,” Journal of Controlled Release., 45, 35-40, 1997.

[31]. JIHUAI WU, CONGRONG WEI, et al., “Influence of the COOH and COONa groups and crosslink density of poly(acrylic acid)/montmorillonite superabsorbent composite on water absorbency,” Polymer International., 50, 1050-1053, 2001.

[32]. AJAMAN ADAIR, PAIROTE KLINPITUKSA, AZIZON KAESAMAN., “Influences of neutralization of superabsorbent hydrogel from hydroxyethyl cellulose on water swelling capacities,” AIP Conference Proceedings., 1868, 020012, 2017.

[33]. OGUZ OKAY, MANFRED KURZ, KARIN LUTZ, WERNER FUNKE., “Cyclization and reduced pendant vinyl group reactivity during the free-radical cross-linking polymerization of 1,4-divinylbenzene,” Macromolecules., 28, 2728-2737, 1995.

[34]. K. SUNITHA, R. SADHANA, DONA MATHEW, C.P. REGHUNADHAN NAIR., “Novel superabsorbent copolymers of partially neutralized methacrylic acid and acrylonitrile: characteristics,” Designed Monomers and Polymers., 18, 512-523, 2015.

[35]. PING I. LEE., “Kinetics of drug release from hydrogel matrices,” Journal of Controled Release., 2, 277-288, 1985.

[36]. SEDDIKI NESRINNE, ALIOUCHE DJAMEL., “Synthesis, characterization and rheological behavior of pH sensitive poly (acrylamide-co-acrylic acid) hydrogels,” Arabian Journal of Chemistry., 10, 539-547, 2017.

[37]. JEANNINE E. ELLIOTT, MARA MACDONALD, JUN NIE, CHRISTOPHERN. BOWMAN., "Structure and swelling of poly (acrylic acid) hydrogels: effect of pH, ionic strength, and dilution on the crosslinked polymer structure," Polymer., 45, 1503-1510, 2004.

[38]. SUDA KIATKAMJORNWONG, PATTAMA PHUNCHAREON., "Influence of reaction parameters on water absorption of neutralized poly(acrylic acid-co-acrylamide) synthesized by inverse suspension polymerization," Journal of Applied Polymer Science., 72, 1349-1366, 1999.

[39]. MINGZHU LIU, RUI LIANG, LAFU ZHAN, ZHAEN LIU, AND AIZHEN NIU., "Preparation of superabsorbent slow release nitrogen fertilizer by inverse suspension polymerization," Polymer International., 56, 729-737, 2007.

[40]. YUHONG ZHANG, LENING WANG, XIAOHONGLI, PEIXIN HE., "Salt-resistant superabsorbents from inverse-suspension polymerization of PEG methacrylate, acrylamide and partially neutralized acrylic acid," J. Polym. Res., 18, 157-161, 2011.

[41]. NOHA MOHAMED ABD EL-SALAM DEGHIEDY., "Synthesis and characterization of superabsorbent hydrogels based on natural polymers using ionizing radiations," Thesis Al-Azhar University, 2004.

[42]. ZUMING JIANG, XULONG CAO, LANLEI GUO., "Synthesis and swelling behaviour of poly (acrylic acid-acryl amide-2-acrylamido-2-methy-propansulfonic acid) superabsorbent copolymer," J Petrol Explor Prod Technol., 7, 69-75, 2017.

[43]. K. SUNITHA, R. SADHANA, DONA MATHEW, REGHUNADHAN NAIR., "Novel superabsorbent copolymers of partially neutralized methacrylic acid and acrylonitrile: synthesis, characterization and swelling characteristics," Designed Monomers and Polymers., 18, 512-523, 2015.

[44]. KI HYUN KIM, DAISUKE SHINDO, et al., "Charging effects on SEM/SIM contrast of metal/insulator system in various metallic coating conditions," Materials Transactions., 51, 1080-1083, 2010.

[45]. MARIA FERNANDA ESCORIZA, PATRICK J. TREADO, et al., "Raman spectroscopy and chemical imaging for quantification of filtered waterborne bacteria," Journal of Microbiological Methods., 66, 63-72, 2006.

[46]. AXEL FEY, STEFAN EICHLER, CARLOS A. GUZMAN, et al., "Establishment of a real-time PCR-based approach for accurate quantification of bacterial RNA Targets in water, using salmonella as a model organism," Applied and Environmental Microbiology., 70, 3618-3623, 2004.

[47]. LINDSAY SOH, MAHDOKHT MONTAZERI, JULI B. ZIMMERMAN, et al., "Evaluating microalgal integrated biorefinery schemes: Empirical controlled growth studies and life cycle assessment," Bioresource Technology., 151, 19-27, 2014.

[48]. CHAOYANG WEI, YUN HUANG, YAHUI SUN, et al., "The kinetics of the polyacrylic superabsorbent polymers swelling in microalgae suspension to concentrate cells density," Bioresource Technology., 249, 713-719, 2018.